energies

MDPI

Article

Simulation-Based Comparative Assessment of a Multi-Speed Transmission for an E-Retrofitted Heavy-Duty Truck

Milla Vehviläinen [1,*], Pekka Rahkola [1], Janne Keränen [1], Jenni Pippuri-Mäkeläinen [1], Marko Paakkinen [1], Jukka Pellinen [2], Kari Tammi [3] and Anouar Belahcen [4]

1 VTT Technical Research Centre of Finland Ltd., P.O. Box 1000, FI-02044 Espoo, Finland; pekka.rahkola@vtt.fi (P.R.); janne.sami.keranen@vtt.fi (J.K.); jenni.pippuri-makelainen@vtt.fi (J.P.-M.); marko.paakkinen@vtt.fi (M.P.)
2 Independent Researcher, FI-33100 Tampere, Finland; jukkatpellinen@gmail.com
3 Department of Mechanical Engineering, Aalto University, FI-02150 Espoo, Finland; kari.tammi@aalto.fi
4 Department of Electrical Engineering and Automation, Aalto University, FI-02150 Espoo, Finland; anouar.belahcen@aalto.fi
* Correspondence: milla.vehvilainen@vtt.fi

Abstract: Electric retrofitting (e-retrofitting) is a viable option for accelerating the renewal of heavy-duty vehicle fleets to reduce the related emissions. We introduce a simulation-based assessment of e-retrofitting strategies for heavy-duty vehicles. Our simulation tool, an electric vehicle fleet simulation toolbox, comprises three modules, namely driving cycles, vehicle dynamics, and vehicle profiles. The first allows for the creation of realistic driving cycles based on GPS data from real routes. The vehicle dynamics and vehicle profiles incorporate, e.g., the modelling of the powertrain and driving conditions. Ten realistic driving cycles were created and used for investigating and comparing three different powertrain alternatives, including the original diesel powertrain, electric with a single-speed transmission and electric with a multi-speed transmission. The vehicles were simulated in two different heavy-load scenarios. First, driving with a cargo load represented by the maximum vehicle weight and second, driving with snow ploughing. We found that the multi-speed transmission in an electric heavy-duty truck significantly improved its traction performance and gradeability. On the other hand, the effect on the electric powertrain efficiency, and thereby on the energy consumption, remained rather minor. Considering the given workload scenarios, our results advocate employing rather than omitting the gearbox in the e-retrofit truck process.

Keywords: vehicle simulation; heavy-duty truck; e-retrofit; electric powertrain; duty cycle; driving cycle; driving performance; single-speed; multi-speed; transmission

Citation: Vehviläinen, M.; Rahkola, P.; Keränen, J.; Pippuri-Mäkeläinen, J.; Paakkinen, M.; Pellinen, J.; Tammi, K.; Belahcen, A. Simulation-Based Comparative Assessment of a Multi-Speed Transmission for an E-Retrofitted Heavy-Duty Truck. *Energies* **2022**, *15*, 2407. https://doi.org/10.3390/en15072407

Academic Editors: Dimitrios Koulocheris and Chunhua Liu

Received: 24 February 2022
Accepted: 23 March 2022
Published: 25 March 2022

1. Introduction

The majority of commercial heavy-duty vehicles in the EU are powered by diesel engines [1] having consequently a big impact on the energy consumption and emissions produced from road transport [2]. The heavy-duty vehicles account for about 25% of transport related CO_2 emissions and 6% of the total emissions in EU [3]. There is a vast incentive to reduce both the energy consumption and emissions of this particular sector, electrification being one of the solutions. Although major players, such as Volvo, Scania and MAN, have initiated a comprehensive portfolio of electrical alternatives in general, the renewal of the heavy-duty fleets is still in its initial stage. The reasons for this are the long lifetimes of existing vehicles, and partly also the availability and performance of the present technologies.

One option for speeding up the fleet renewal process is retrofitting the internal combustion engine (ICE) vehicles with an electric powertrain. Electric retrofits (e-retrofits) have gained a lot of attention in recent years and there are companies offering commercial retrofitting kits for heavy-duty vehicles. For example, Linkker has launched a retrofit kit

called LinkDrive [4] and Pepper Motion offers e-troFit concept [5], both specialised for heavy-duty buses. Notably, the e-retrofit cases of heavy-duty vehicles tend to focus on fleet buses predominantly because the driving cycles and performance requirements are usually more predictable for transit buses than they are for commercial trucks. Retrofitting ICE vehicles potentially increases acceptance and adoption of electric vehicles [6]. It offers a more cost-efficient and sustainable alternative to new hardware [7], which not only increases the resource utilisation of ICE vehicles [6] but also extends the lifetime of the current fleets on the market and accelerates the electrification of the current vehicles on the streets.

Electric powertrains are often equipped with single-speed transmissions due to the high performance of electric motors over a large speed range. Their simple structure also mitigates cost, volume, energy losses and the overall drivetrain mass [8]. However, with commercial heavy-duty trucks supplemental driving resistance is caused by high gross vehicle weights, varying route grade and different terrain types. Thus, it may be necessary to ensure a proper traction performance with a gearbox. Additional gear ratios allow the motor to work in its most efficient operating range. Better efficiency appears as higher top speed, faster acceleration and increased gradeability [8]. Besides, it reduces the power requirement of the motor and drains less power from the battery leading to an increased driving range or reduced battery size [9].

Multi-speed transmissions designed for electric heavy-duty vehicles have also attracted attention in the related literature. Ahssan et al. [8] review and analyse recent studies of electric vehicle (EV) transmissions and find clear benefits when comparing both dynamic and economic performances between electric single-speed and multi-speed vehicles. As it is a gradual process to design and build a new powertrain, most of the recent studies apply different simulation methods to anticipate and evaluate the feasibility of certain configurations beforehand. Simulations typically employ basic vehicle physics to describe driving of a particular vehicle on a given route, modelled as a driving cycle. Since generating driving cycles from scratch is laborious, either standard or computationally created test driving cycles are exploited in many cases.

Morozov et al. [10] simulate five different electric motor models, with the power varying from 150 kW to 350 kW, combined with three to six-speed heavy–duty vehicle powertrain transmissions using MATLAB Advisor. Commonly-known commercial driving cycles produced by a chassis dynamometer were exploited. The authors report that despite the motor power, with more gears higher efficiency regions of motor operation were reached, although the sufficient acceleration could not be achieved with multiple gears alone but when combined with a more powerful motor. Similarly, Verbruggen et al. [11] simulate heavy-duty vehicle energy consumption by comparing a single-speed truck to modified configurations with two, three, and four gears using MATLAB. Their driving cycle was derived from the Vehicle Energy consumption Calculation Tool (VECTO), devised by the European Commission for determining fuel consumption and CO_2 emissions caused by heavy-duty vehicles [12]. Verbruggen et al. [11] find that after the biggest advance from the second gear, more gears would not bring other benefits than gradeability in terms of a more dynamic driving cycle. Tan et al. [13], in turn, exploit a specific driving cycle on a mine construction site. Their paper simulated the optimisation of a two-speed transmission for a dump truck application using MATLAB Simulink and Autonomie. The authors apply an increased rolling resistance together with the ground grade to represent terrain characteristics and find that additional gears improving both the acceleration capability and energy efficiency.

Still, applying multi-speed transmission in an electric powertrain is a moderately new concept. In the previous studies, transmission systems are designed for specific applications, whereupon the main challenge has been optimising the gear ratios and shifting strategies for individual cases [10,13]. In retrofit cases, however, these issues can be neglected since the gear ratios and gear shifting technology of the old powertrain can be exploited as they are. We use this as an advantage. Further, the majority of the papers focus on economic

performance [11,14] and less is known about the dynamic performance under extreme conditions which is our main point of focus.

In this study, we assess the dynamic traction performance of an e-retrofitted heavy-duty truck in high load conditions. We simulate a real case, where a diesel powered heavy-duty truck is e-retrofitted. The simulations are carried out using a special simulation toolbox which we expand for our needs. The original drivetrain transmission, consisting of a six-speed gearbox and a torque converter, can be connected to an electric powertrain. By comparing the single-speed to the multi-speed configuration, we evaluate the benefit from retaining the existing transmission.

We simulate two types of driving scenarios, namely a cargo load represented by the maximum vehicle weight and snow ploughing realised by increased rolling resistance. To our best knowledge, no prior simulations are run for varying loading cases where phenomena such as snow ploughing is demonstrated. Simulation parameters for three different vehicle profiles are specified. The profile types are the original diesel, electric single-speed and electric multi-speed powertrain. Each vehicle profile is simulated in both load conditions, resulting in six simulation cases in total.

A novel approach to create realistic driving cycles by combining road and map data is also implemented. Our simulation tool is used to determine ten driving cycles harnessing experimental GPS data gathered from typical driving routes of the studied truck. The research makes the following contributions:

1. Introducing a simulation platform capable for electric and diesel powered multi-speed trucks;
2. Creation of representative driving cycles based on real driving route map data;
3. Evaluation of benefits from additional gears to driving performance of an electric truck.

The article is organised as follows. Section 2 introduces the simulation methods and our case parameters. In Section 3, the resulting traction description, transmission control, map-based driving cycles, realised speed performance, powertrain efficiency, and energy consumption outcomes are examined. The discussion and final conclusions are presented in Section 4.

2. Simulation Framework

We simulate the dynamic performance of a heavy-duty truck using VTT Smart eFleet (SeF) simulation toolbox [15] which employs a multi-physics approach to analyse the energy flow in electric vehicle systems. SeF was originally developed for electric bus fleets, but has subsequently been implemented for other vehicle types as well. With the developed methodology, it is possible to analyse varying vehicle profiles, operation environments and infrastructures by taking geographical aspects, such as topography, into account alongside mechanical and electrical capabilities. The toolbox has been validated, for instance, in realistic heavy-duty operation cases for electric buses using measured data from a chassis dynamometer [16] and real-life [17,18] experiments.

For the current work, SeF is expanded further to be applicable in heavy-duty truck simulations. We advance the existing functionalities and combine them with new models of a diesel engine, automatic multi-speed transmission and torque converter. The simulation scope is also augmented with a traction performance study to estimate the tractive capability required from the powertrain system due to heavy load working cycles.

The simulation environment encompasses three main modules which are covered in the following Sections 2.1–2.3. Figure 1 visualises the whole simulation process. The route module stores the geographical information and creates the driving cycles. Similarly, the vehicle module stores multiple vehicle profiles that describe the specifications for each simulation scenario. Together these modules input vehicle profile and driving cycle properties to the simulation module which provides the vehicle dynamics.

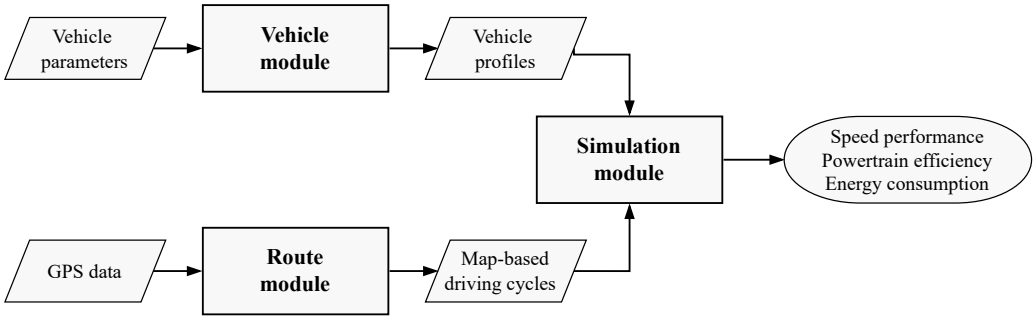

Figure 1. Flowchart presentation of the whole simulation process.

2.1. Driving Cycle Creation

SeF incorporates a novel way to create driving cycles based on real map data. This methodology is analysed, as an example, in Anttila et al. [18]. The route shape formed from the geographical data is elaborated further to obtain a more detailed digital description of the routes. The process starts from defining the shape for a particular route. Each route is divided into short segments constructed from a list of coordinates. The coordinates are derived either manually or automatically using a geographical information system. Length of segments define the distance of the route and angles between them describe curvatures along the route. In addition to the route shape parameters, the other properties such as speed limit and road slope are carried out separately based on the geographical map information.

The final speed profile of a driving cycle is completed through simulation algorithms which modify the original speed limit taking into account crossroads, route curvatures, and other route characteristics. For example, if the speed limit is 40 km/h on a given road segment and the vehicle takes a turn to the right, the realised driving cycle speed request is much lower compared to the speed limit before, during and after the turn. The given methodology allows us to determine realistic driving speeds for a large set of driving cycles.

2.2. Vehicle Dynamics

The simulation module employs basic vehicle longitudinal dynamics to simulate traction performance of heavy-duty vehicles. The equations of motion of the truck while moving follows Newton's II law (1):

$$F_{tr} - F_d - F_r - F_g = M\dot{v}, \tag{1}$$

where F_d, F_r, F_g and F_{tr} are the force components describing aerodynamic drag resistance, rolling resistance, gradient resistance and tractive force, respectively. In addition, M is the total vehicle mass and $\dot{v}$ represents acceleration, the first derivative of speed. The realised speed of the vehicle is carried out from Equation (1) via time integration.

The aerodynamic drag resistance takes into account the effect of air resistance (2):

$$F_d = \frac{1}{2} \cdot \rho \cdot C_d \cdot A \cdot v^2, \tag{2}$$

where ρ, C_d, A and v denote constant parameters for the air density, aerodynamic drag coefficient, frontal area of the vehicle and its speed, respectively.

Rolling resistance force presents the force required to overcome the rolling resistance affecting the tires (3):

$$F_r = C_r \cdot M \cdot g \cdot cos(\theta), \tag{3}$$

where C_r and g stand for the rolling resistance coefficient and acceleration of gravity. θ denotes the road slope angle.

In turn, the gradient resistance from the route grade describes the force needed for an incline or decline slope (4):

$$F_g = M \cdot g \cdot sin(\theta). \tag{4}$$

Finally, the traction force on the wheels is calculated through the transmission parameters (5):

$$F_{tr} = T \cdot \frac{i_g \cdot i_{fd} \cdot \eta_f}{r_w}, \tag{5}$$

where T is the motor torque, r_w denotes the dynamic radius of the wheels, i_g and i_{fd} are the gear ratio and final drive ratio. η_f is the constant driveline efficiency coefficient determined by the final drive for a single-speed and by the final drive and gearbox for multi-speed versions.

We use the existing electric motor functionality in SeF, which is previously reported for example by Halmeaho et al. [16]. The electric motor is rigidly connected to the transmission with the locked torque converter so the motor speed is always proportional to the vehicle speed through the given gear ratio. Consequently, the electric motor and transmission consistently share the same rotational speed which is calculated from the dynamic radius of the wheels (6):

$$\omega_{locked} = i_{fd} \cdot i_g \cdot \frac{v}{r_w}. \tag{6}$$

As the latest amendment to our simulation tool SeF, the diesel powertrain from the engine to the transmission was modelled. Apart from the electric powertrain, the diesel engine model implementation needs to reckon that while the torque converter is unlocked, the diesel motor speed is not directly conveyed to the powertrain. For this reason, the separate equation of motion is needed for the engine crankshaft (7):

$$T_{eng} - T_{res} - T_{conv} = J_{eng}\dot{\omega}, \tag{7}$$

where J_{eng} is the total inertia of the engine rotating mass and ω represents the angular acceleration, the first derivative of the engine crankshaft rotation speed. T_{eng} and T_{res} are the driving torque acting on the crankshaft and the resistive torques including the friction and pumping losses, respectively. The resistive forces are considered as a viscous load. T_{conv} denotes the torque acting on the converter input axle (8):

$$T_{conv} = \frac{\omega^2}{K^2}, \tag{8}$$

where K denotes the converter capacity factor between the torque output and input speed. The capacity factor is dependent on the speed ratio as well as the torque ratio, which describe the ratio of speed and the torque between the converter input and output axle, respectively.

The torque converter is controlled so that when starting from a standstill the converter is unlocked and a constant rotation speed is requested from the diesel engine. This occurs always in the first gear. When the output speed of the converter is close to the engine speed, the converter is locked until the vehicle speed is almost zero. That is, with the diesel truck simulations the torque converter is unlocked only at slow speeds at starting and stopping situations. Otherwise the rotational speed is calculated as in Equation (6).

2.3. Vehicle Profiles

Figure 2 depicts simplified powertrain configurations of three different vehicle types. The first configuration, denoted by D6s, is the original truck with the diesel engine and six-speed automatic transmission including the torque converter. D6s also includes a final drive which is used in both electric powertrains as well. The e-retrofitted single-speed

version is shown in the second configuration which is referred to as E1s. Its electric driveline consists of an electric motor, battery pack, inverter and the final drive. The third powertrain type is composed by combining the electrical components and the original multi-speed transmission with the locked torque converter so the motor speed is always proportional to the vehicle speed through the given gear ratio. This configuration is named E6s.

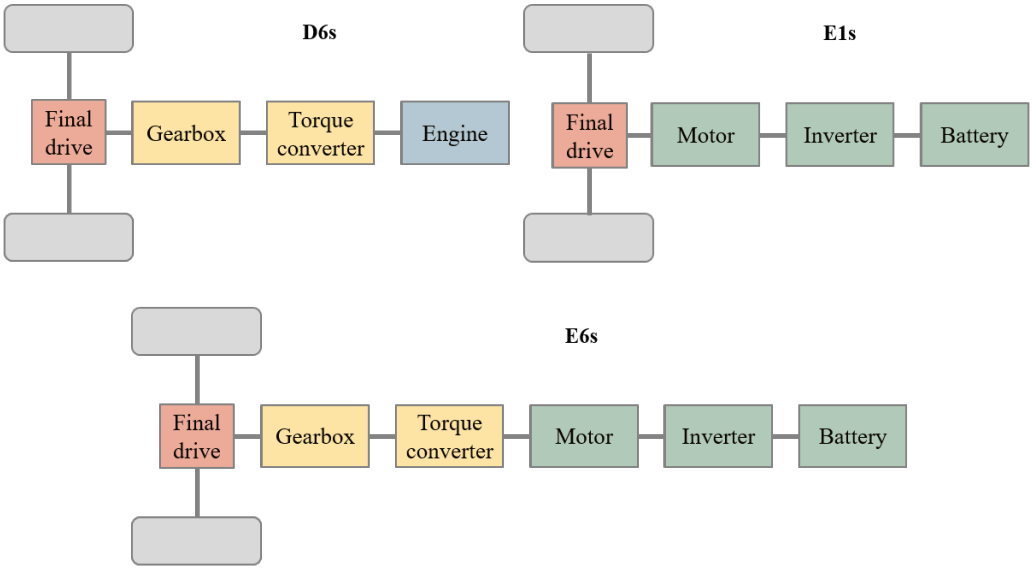

Figure 2. Three powertrain configurations used in the simulations.

Our simulation work is based on a real e-retrofit case performed by Tampere University of Applied Sciences for a vehicle of Helsinki City Construction Services (Stara) with funding via Forum Virium Helsinki Ltd. All participating organisations locate in Finland. The commercial heavy-duty vehicle considered in this study is a three-axle diesel truck with one driven axle (6 × 2 axle configuration) from 2013 (Figure 3). It has a conventional ICE powertrain with a six-speed automatic gearbox with a torque converter. The truck is equipped with a cable lift system, which enables the attachment of different bodywork making it a multipurpose utility vehicle suitable for a large variety of work cycles. Typical work cycles include road maintenance work and municipal utility work within fixed regions, daily driving ranges, and changing loading conditions. The specification parameters of the original vehicle are listed in Table 1.

Table 1. Technical specification of the original diesel truck.

Technical Parameter	Value
Gross vehicle weight	15,000 kg
Maximum vehicle weight	28,000 kg
Wheelbase	4.0 m
Tyre radius r_w	0.53 m
Frontal area A	6.9 m^2
Inertia coefficient	1.035
Drag coefficient	1.0
Rolling resistance coefficient	0.006
Max. power @ 1900 rpm	235 kW (320 hp)
Max. torque	1600 Nm
Gear ratios 1–6	3.49; 1.86; 1.41; 1; 0.75; 0.65
Final drive ratio	4.85
Torque converter	Yes
Gearbox efficiency	0.98
Final drive efficiency	0.96

Figure 3. The original diesel truck to be e-retrofitted, together with the removed diesel engine in the lower right corner. Photo credit: Ruska Tapiovaara, Forum Virium Helsinki Ltd., Helsinki, Finland.

The diesel engine has a maximum power output of 235 kW and a maximum torque of 1600 Nm. The left graph in Figure 4 describes the engine torque and power curves with respect to the rotational speed. The total efficiency coefficient for the diesel powertrain is 0.94, which is a product of the general gearbox and final drive efficiencies [19]. The fuel consumption of the engine is modelled as a function of the engine speed and respective load. The fuel rate map is derived from a specific fuel consumption map that has a generic shape and the lowest specific fuel consumption value of 192 g/kWh. Figure 5 shows the resulting fuel rate map, based on which the diesel vehicle consumption is carried out in the simulations.

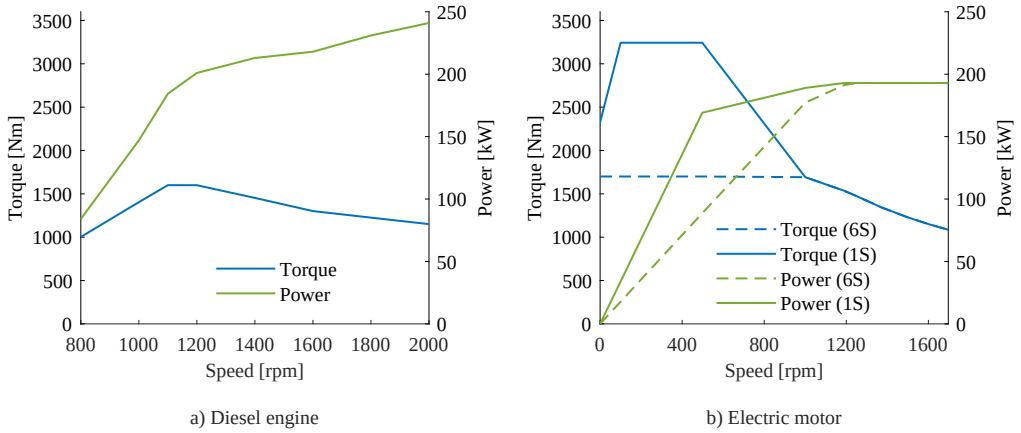

a) Diesel engine b) Electric motor

Figure 4. (**a**) Torque and power curve of the diesel engine. (**b**) Torque and power curve of the electric motor, where the both are limited according to the maximum input torque of the gearbox for the multi-speed profile.

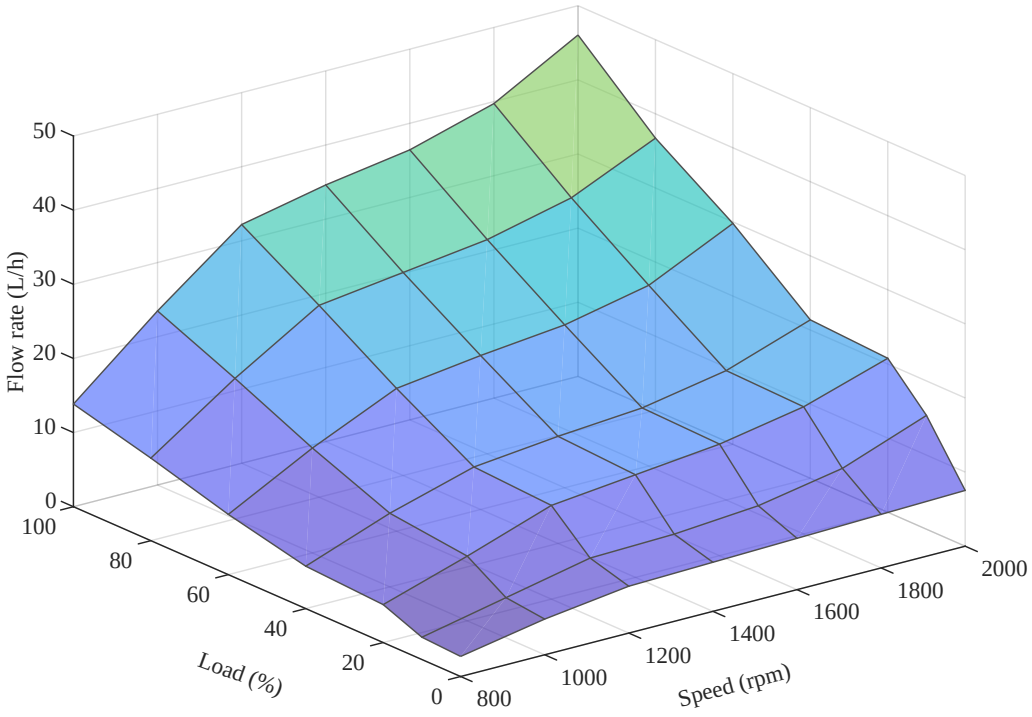

Figure 5. Fuel rate map of the diesel engine.

In the electric retrofit version, the diesel engine and fuel tank are replaced by electrical components, including an electric motor, inverter and battery pack. The electric motor used in the both electric trucks is selected so that its power is within the same range as the diesel engine power. The battery pack is selected to have a slightly higher maximum power compared to the nominal motor power. Table 2 lists the principal parameters of the electrical components used for the retrofitted powertrain. However, it is important to note that the battery capacity is fairly irrelevant at this point as the simulated distances are expected to be short enough to be run without considering recharging. We use a constant battery voltage in our simulations. The battery energy is calculated by integrating the battery power, which is defined using the battery voltage and current. Effects from other auxiliary devices are excluded from the vehicle model for the sake of simplicity. The total efficiency coefficient for the e-retrofitted multi-speed powertrain is the same 0.94 as for the diesel version. For the single-speed the efficiency is 0.96 according to the final drive efficiency [19].

Table 2. Technical specification of the electric driveline components.

Technical Parameter	Value
Motor nominal power	177 kW
Motor nominal speed	1200 rpm
Battery size	400 kWh
Battery voltage	700 V
Battery max. continuous current	277 A
Battery max. continuous power	194 kW
Battery resistance	0.13 Ω

Both the electric motor and battery can provide temporary peak power for short periods, the motor over the nominal power of 177 kW and the battery over 194 kW. However, this may lead to overheating without a proper control of the temperatures. The party performing the converting work has decided not to overload the battery for safety reasons,

and therefore they have limited the battery current to 277 A (Table 2). We also choose not to overload the battery and to limit the motor overloading to the battery power, since the detailed battery and thermal modelling of the motor are omitted in this study. In our case, the corresponding maximum battery power of 194 kW limits the overloading of the motor up to 10%. Besides, in snow ploughing, continuous power is required and peak power would offer only minor benefit. The torque and power curves of the electric motor are plotted to the right graph of Figure 4 where the motor power limitation according to the battery power is taken into account.

The distinctive phenomenon here is that, unlike an ICE, an electric motor can provide torque from zero speed. Regardless, the output torque is different for cases with and without a gearbox. In former, a zero speed cut from zero to 100 rpm due to overheating protection is set since the electric single-speed with a constant final drive ratio cannot advance the maximum torque when starting from a standstill. That is, the starting torque is smaller compared to the maximum torque while driving. In the latter, the starting torque cut is unnecessary due to the gearbox torque limitation. Since the gearbox cannot take in more than 1700 Nm torque, the motor torque is limited accordingly for the multi-speed powertrain, which is also taken into account in Figure 4.

Typical efficiency values of an electric motor are used to derive the electric powertrain efficiency with respect to the rotational speed of the motor and the corresponding load. The efficiency is defined for the motor-inverter set-up. Figure 6 visualises the efficiency map used for simulating electric vehicle types. The load is normalised by the nominal torque of the electric motor and therefore the electric drive can produce torque over its nominal value, but to note, in our case overloading is limited by the battery characteristics.

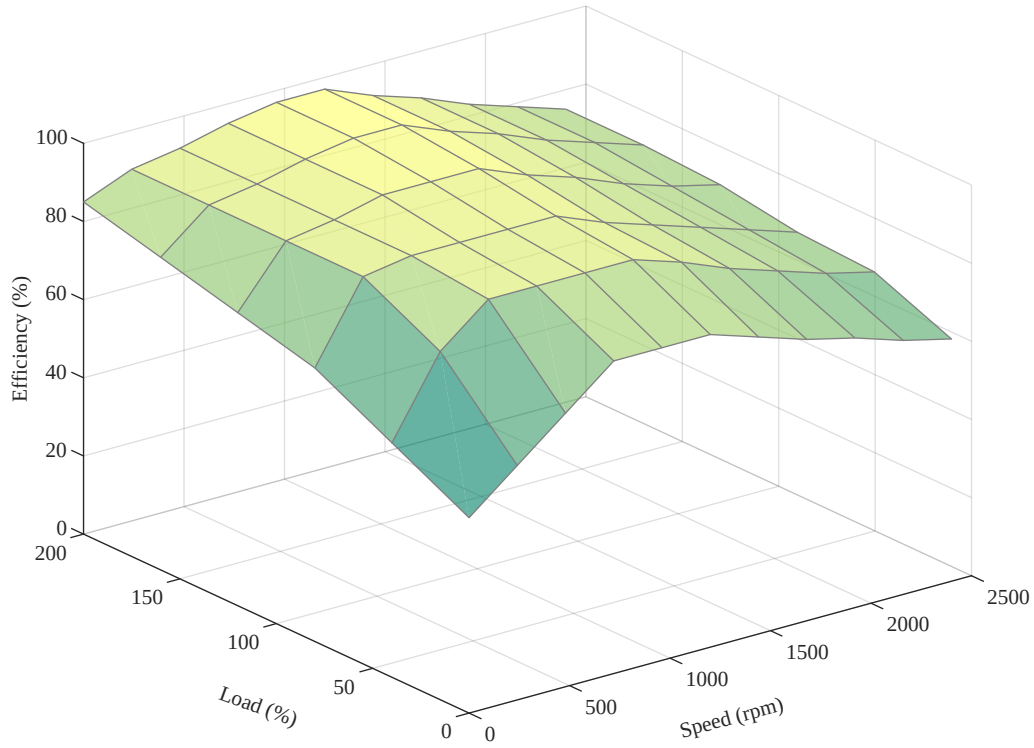

Figure 6. Efficiency map of the electric motor and inverter set-up.

All three powertrain configurations are simulated with two different load scenarios, resulting in six separate simulation cases. The cargo load profiles represent the truck with its maximum mass, whereas the snow load profiles represent the corresponding version with additional driving resistance from snow ploughing, but with a smaller overall mass. The load case description is added to the vehicle profile denotation (either with 'cargo' or 'snow').

The maximum allowed gross vehicle weight, 28 tons, for a three-axle heavy truck in Finland is used for the cargo load profile. Electric vehicles typically weigh more than diesel vehicles due to the added mass of the batteries, but as the maximum weight limit applies despite the vehicle type the maximum gross vehicle weight of the electric cargo truck is the same as the diesel profile. For all snow load profiles, we use a typical mass of 20 tons. The mass of additional working equipment is included in this total mass value. In reality, the total vehicle mass usually varies throughout the driving cycles, but we use constant masses throughout the simulations to emphasise extreme driving conditions. Keeping the total weight of different profiles the same also alleviates comparison of the final results. To clarify, the total vehicle mass is specified only according to the load case, not by the difference in technical gear.

The rolling resistance coefficient is a central parameter for the resulting traction force and for typical heavy-duty trucks it varies between 0.004–0.007 [20]. We use an average value of 0.006 for all cargo load profiles. Then again, snow ploughing causes an additional driving resistance which is simulated by increasing the rolling resistance. We have measured data about the consumption of the diesel vehicle while under a heavy snow load. The average consumption was approximately 80–100 L per 100 km. The driving resistance in snow load scenarios is determined by increasing the rolling resistance coefficient of the reference profile until, with a 20,000 kg mass, it results in a similar average consumption than what was initially given. This occurs when the rolling resistance is set to 0.05. These main vehicle profile parameters for determining the load cases are listed in Table 3.

Table 3. Varying vehicle profile parameters.

Profile Notation	Mass	Roll. Res. Coeff.	Transmission
D6s_cargo	28,000 kg	0.006	6-speed gearbox with torque converter
E1s_cargo	28,000 kg	0.006	single-speed
E6s_cargo	28,000 kg	0.006	6-speed gearbox with torque converter
D6s_snow	20,000 kg	0.05	6-speed gearbox with torque converter
E1s_snow	20,000 kg	0.05	single-speed
E6s_snow	20,000 kg	0.05	6-speed gearbox with torque converter

The vehicle profiles are simulated either with the single-speed or multi-speed transmission. In former, there is only the final drive ratio between the electric motor and wheels. The latter is the combination of the gearbox and torque converter, and it also requires modelling of the gear switching logic which we implement by means of the rotational speed limits for the rotating machine end. This is applied to both the ICE and EV powertrains, but with different limiting values. The upper and lower limits for the diesel engine are 1800 and 1200 rpm, respectively. The corresponding values for the electric motor are 1600 and 800 rpm. As it can be seen from Figure 4, the motor power between these rotational speeds is at its maximum. When the rotational speed drops below the lower limit, the gear is upgraded and when the nominal speed is reached, the gear is reduced. The limits were selected so that there would be enough power available for the traction. Thus, the control logic is not primarily optimised to get the lowest possible energy consumption.

At this point, the torque converter between the motor and the gearbox is taken into account by modelling its locking logic for the diesel version only. The gear transmission and torque converter physics are transferred from the diesel vehicle to the electric multi-geared powertrain as they are, but the locking logic is dropped since it is not yet decisive.

3. Results

The starting point for our results is the description of the traction performance of the diesel and electric powertrains. Traction graphs provide a general overview of what kind of performance can be expected with the given traction motors and transmission systems. Next, the effect of a transmission control on the vehicle acceleration is examined with a demonstration of the gear switching logic. We also present the map-based driving

cycles carried out, followed by a comprehensive analysis of the realised speed, powertrain efficiency and energy consumption results of the studied vehicle types.

3.1. Traction Performance

The traction performance of the truck is assessed using the tractive force graph, which presents the availability of tractive forces over the whole speed range of the vehicle operations. The graph describes the capabilities of starting from standstill, hill climbing and driveability over the speed range so that there is enough force available for sudden acceleration. When a vehicle starts from a standstill, it cannot benefit from kinetic energy and therefore more traction is required compared to regular driving. Figure 7 shows tractive force graphs for the diesel powertrain (on the left) and for electric powertrains including the single-speed and the six-speed gearbox (on the right), all having the maximum mass of 28 tons.

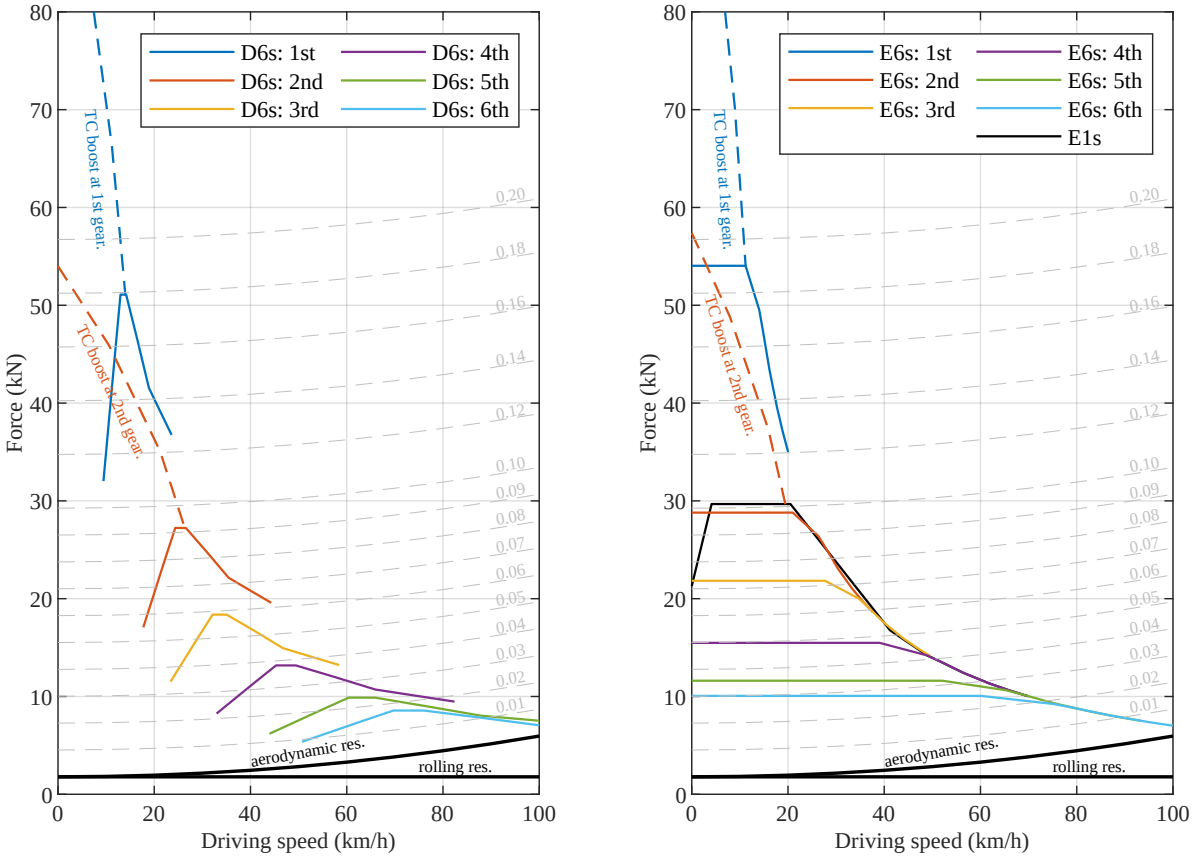

Figure 7. Tractive force curves for the diesel (on the left) and electric (on the right) powertrains. The grey dashed lines represent road slopes in per cent whereas the solid coloured lines show the tractive forces in each gear. The blue and red dashed lines represent the available maximum torque when the converter is unlocked in the first and second gear, respectively.

The maximum available tractive force of the diesel version in the first gear and with the locked torque converter is enough to climb an 18% slope at 14 km/h. The dashed lines in the traction graph (Figure 7) show the effect of the torque converter. With the diesel version, the zero-speed traction force reaches about 100 kN and 55 kN in the first and second gear, respectively. At 80 km/h highway speed, there is enough traction in the truck to overcome a 1.5% slope in fifth or sixth gear. Then the respective engine load in sixth gear is around 40% and engine rotational speed is 1260 rpm, enabling operation in a high efficiency area. Even a 2% slope is possible at the highway speed in fourth gear. The traction performance of the truck with the diesel engine and the six-speed gearbox is

considered as the reference as this dimensioning is shown to provide sufficient capabilities for climbing, pulling away from a slope and soft terrains, and highway driving.

With the electric multi-speed version, the respective traction values are slightly higher in the small gears. The maximum tractive force in first gear is 54 kN, which is available already at zero speed enabling a pull away from a 19% hill. Then again, the battery power of 194 kW slightly limits the tractive forces at highway speeds. In fifth or sixth gear, accordingly, the electric multi-speed is able to climb the same 1.5% slope at 80 km/h than the diesel version, but in fourth gear the 2% slope is possible only at 70 km/h.

For the electric single-speed configuration without the gearbox, a separate limitation of the motor torque needs to be introduced to prevent overheating. This zero-speed cut in the traction force of the single-speed and the lower maximum tractive force are the main differences when compared to the electric multi-speed transmission. The multi-speed version is able to start from a 19% hill in the first gear while the single-speed truck barely starts from a 7% uphill. Moreover, the maximum hill climbing capability without the gearbox is around 10% with the corresponding 30 kN maximum tractive force. Nonetheless, these numbers are relatively low and make the single-speed truck infeasible for many use cases.

A gearbox, designed for diesel engine use, connected with an electric motor with a larger operational speed range compared to the engine is likely to have redundant gear ratios. In terms of traction performance, the third and the sixth gear could be skipped. Without these gears there would still be enough traction for the whole driving speed range. Nevertheless, additional gears can be exploited to run the electric motor on a more optimum operation point taking into account the current speed and loading conditions. Furthermore, the electric powertrain traction graph (Figure 7, right) includes the dashed lines to illustrate the possibility to generate extra torque by unlocking the torque converter. The torque converter in an electric vehicle powertrain is normally considered unnecessary as electric motors can offer torque from a zero speed. Additionally, electric motors also naturally offer higher tractive forces compared to an ICE with the same nominal power. In the e-retrofit situation, however, the transmission configuration is fixed by the existing components. The gearbox and torque converter in the diesel powertrain are designed to function together and therefore, they cannot be separated. We acknowledge that the converter can be unlocked as a secondary option if needed, but in our simulation case it is considered locked.

3.2. Transmission Control

Based on the gear switching rules presented in Section 2.3, the given logic is demonstrated with a separate acceleration cycle in Figure 8, where all three vehicle types with the cargo load accelerate from zero to 80 km/h and then decelerate back to zero speed. Because the single-speed transmission has a constant gear ratio, its rotation speed is directly proportional to the vehicle speed.

Figure 8 also demonstrates different motor characteristics and the difference in the available power. The diesel truck is the first to reach 80 km/h with the most powerful powertrain. On the other hand, at the very beginning electric multi-speed vehicles accelerate faster than the diesel vehicle as a consequence of higher available traction force at slower speeds. Despite the zero speed cut in torque, the electric single-speed is not far behind. However, because of the restriction due to the battery power, the final acceleration of both electric vehicles suffers slightly. This acceleration simulation does not describe the maximum vehicle acceleration, but it demonstrates the gear change logic. To simulate the maximum acceleration and to obtain the full vehicle performance, different tuning for the controllers defining the actual torque values and gear changing parameters would be needed to ensure the maximum output power.

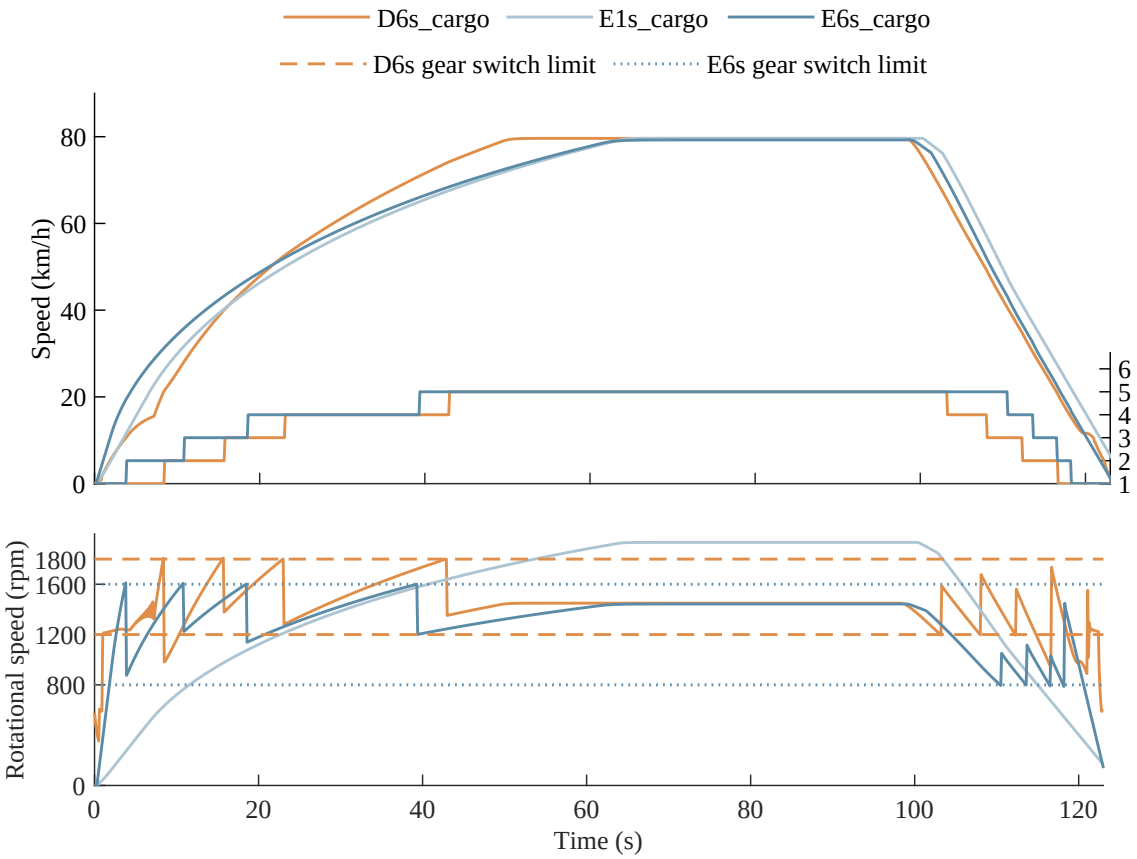

Figure 8. The acceleration cycle with gear changing (**upper graph**) and the corresponding rotational speed (**lower graph**) for the three vehicle types with the maximum mass. Note that E1s_cargo is the single-speed vehicle with a constant gear ratio, which is why its gear changes are missing.

3.3. Map-Based Driving Cycles

The simulations employ experimentally collected GPS data from conventional driving routes, measured with the diesel truck throughout the year 2019, to create the driving cycles. Although a large number of driving cycles can be created quickly, the generated data still requires manual work before it can be used for the simulations. For example, long tunnels may disturb GPS signals and cause biased variations in altitude, which need to be manually adjusted afterwards. Altogether, ten different map-based routes were selected (Table 4) for our purposes.

Table 4. Route profile parameters of the map–based driving cycles.

Route	Length [km]	Slope Max [%]	Slope Min [%]	Ascent [m]	Descent [m]
1	65	13	−13	541	−532
2	40	15	−13	267	−267
3	29	8	−10	167	−161
4	41	8	−8	315	−323
5	23	7	−7	158	−158
6	77	10	−9	630	−629
7	56	12	−12	396	−397
8	40	9	−14	356	−369
9	21	7	−8	165	−173
10	79	15	−10	590	−590

The routes comprehend diverse segments from urban to highway driving. All driving cycles are located in the Helsinki region, the capital area of Finland (Helsinki, Espoo, Vantaa) (Figure 9). Speed limits for heavy-duty trucks in Finland are set to 80 km/h at maximum, which is also considered when generated the driving cycles. These cycles are used for the cargo scenario simulations. For the snow ploughing simulations the driving cycles are modified so that highway speeds of 60–80 km/h are reduced to 60 km/h to give a more realistic model for driving with a snow plough and driving in winter traffic conditions. Figure 10 shows the speed cycles and elevation profiles of the routes with the cargo load.

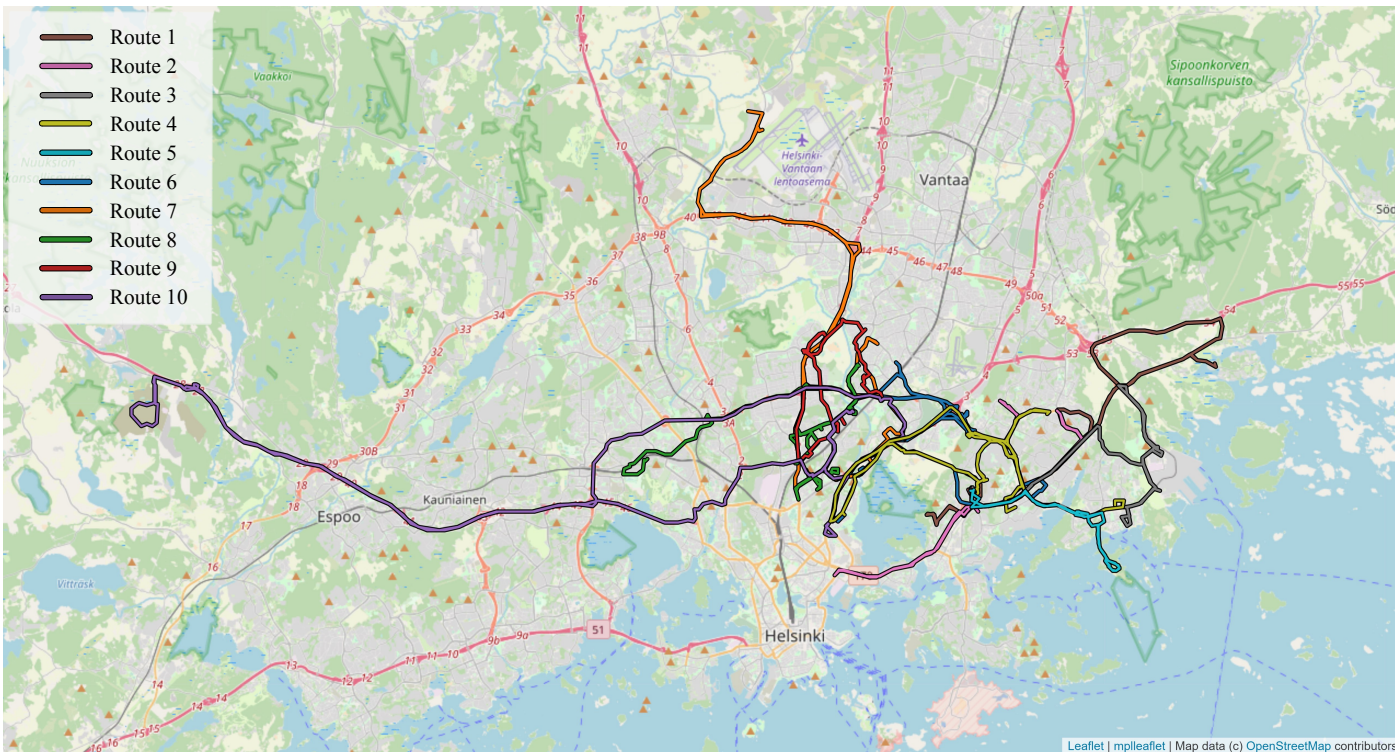

Figure 9. Simulated routes located on the map of the capital area of Finland.

To emphasise the principal outcomes, three routes with different speed and terrain characteristics are used here as examples to report the results. Hence, we refer mostly to routes 5, 8, and 10. The average speed requests of routes 8 and 10 are among the lowest and the highest, respectively. Additionally, Route 5 is considered comparably easier as it is short and variations in its route grades are rather minor.

3.3.1. Speed Performance

Speed performance of a vehicle describes how well it is able to reach and maintain a speed requested by a driving cycle. In addition to the aforementioned acceleration capabilities, the route gradient also has an impact on the speed performance. The realised speed curves for the example routes 5, 8, and 10 with the cargo and snow load are plotted in Figures 11 and 12. The resulted speed curves for all simulations can be seen in Appendix A—with the cargo load in Figures A1 and A2, and with the snow load in Figures A3 and A4.

Figure 11 shows that all vehicle types with the cargo load were able to execute on all routes when the loading was defined by the maximum mass only. The diesel version performed slightly better during longer accelerations. Table 5 also indicates that despite the powertrain configuration, all cargo load profiles had about the same average speed throughout each route. The effect from the acceleration capability of the diesel powertrain to the average speed shows only on routes 2 and 6 where the speed fluctuated the most.

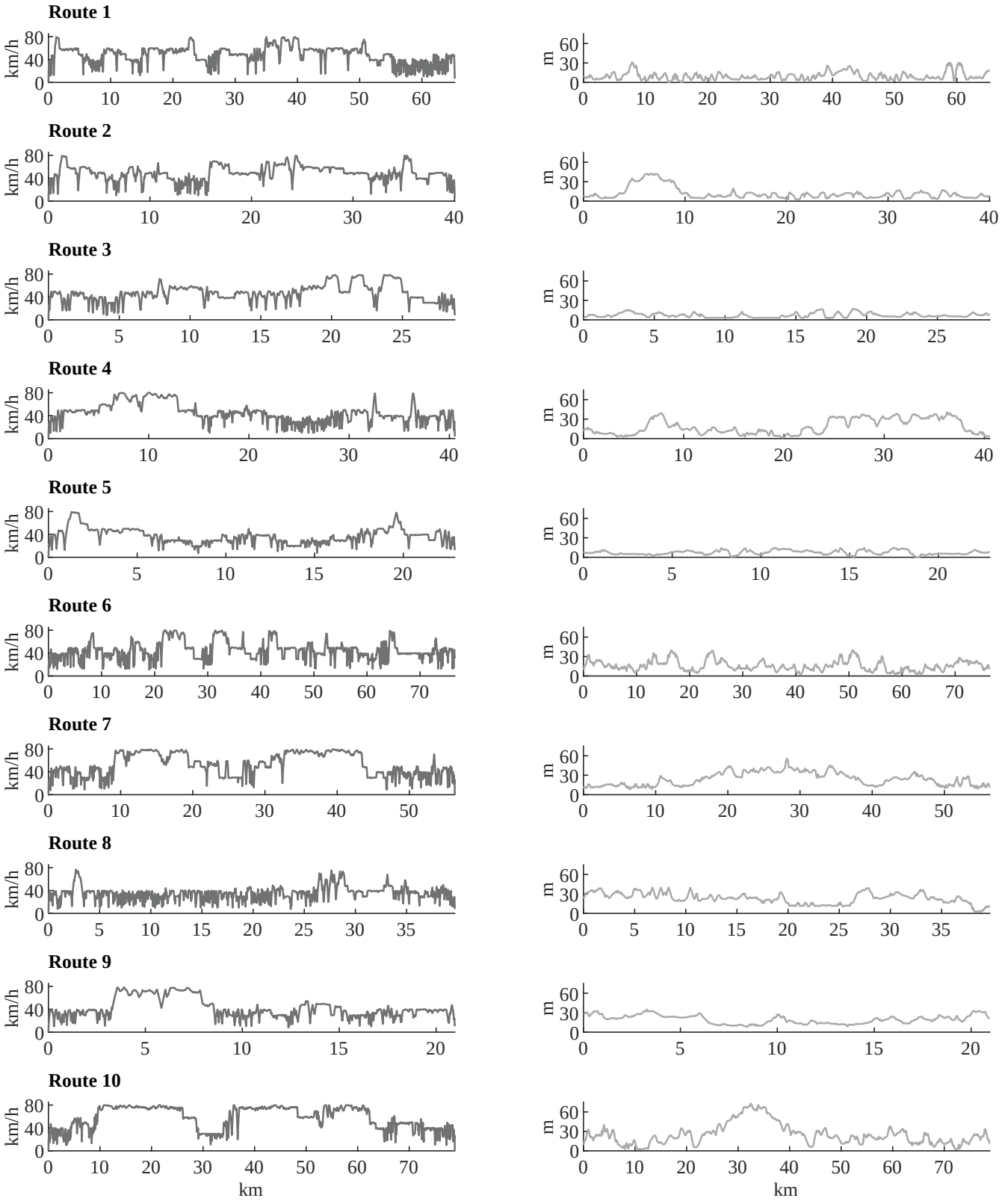

Figure 10. Speed profiles and altitudes of the ten map-based driving cycles. The graphs on the left show the speed profiles and the graphs on the right are the corresponding altitudes.

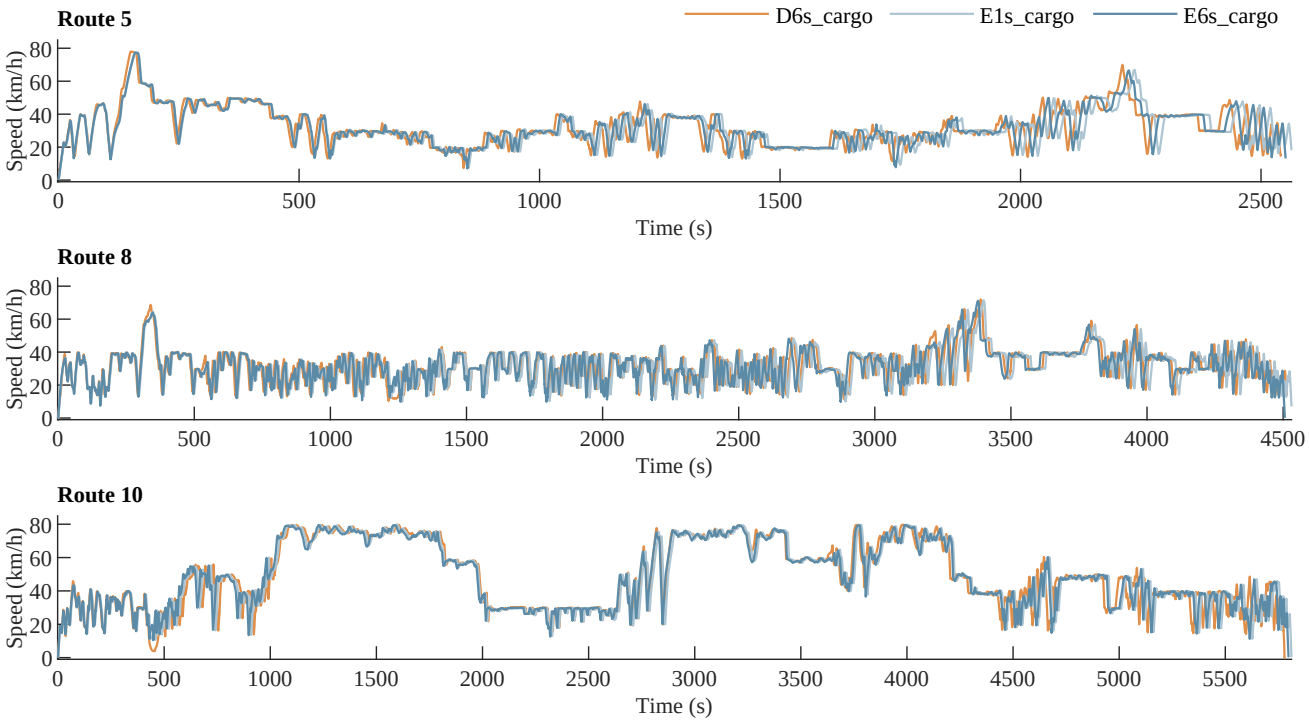

Figure 11. Simulated speeds of three vehicle types with the cargo load on routes 5, 8, and 10.

Differences in the speed performance under a snow load were clearer. Figure 12 shows how the diesel truck is significantly faster than the electric versions whose accelerations are compromised not only by the additional driving resistance from snow but also by the maximum battery power limit. Moreover, the electric single-speed is moderately slower than the multi-speed on routes 5 and 8 (Figure 12). Table 5 shows that the average driving speed of the electric multi-speed truck is slightly higher compared to the single-speed version. This can be explained so that a lack of traction on ascending sections slows down the truck. On Route 10, however, the speed performance of the electric powertrains is almost equal due to the higher average speed that provides kinetic energy to overcome challenging terrain (Figure 12).

Table 5. Average speeds from all simulation runs.

Route	D6s_cargo [km/h]	E1s_cargo [km/h]	E6s_cargo [km/h]	D6s_snow [km/h]	E1s_snow [km/h]	E6s_snow [km/h]
1	42.5	42.1	42.2	40.7	39.1	39.2
2	43.7	43.3	43.3	42.0	40.3	40.3
3	41.2	40.8	40.9	39.7	38.3	38.4
4	39.1	38.8	38.9	37.1	36.1	36.3
5	32.4	32.2	32.3	31.8	31.0	31.5
6	39.6	39.3	39.4	37.9	36.6	36.7
7	44.1	43.7	43.8	40.5	38.6	38.8
8	31.7	31.6	31.7	30.8	30.3	30.6
9	35.5	35.3	35.5	34.0	33.3	33.7
10	49.1	48.8	48.9	43.8	41.5	41.5

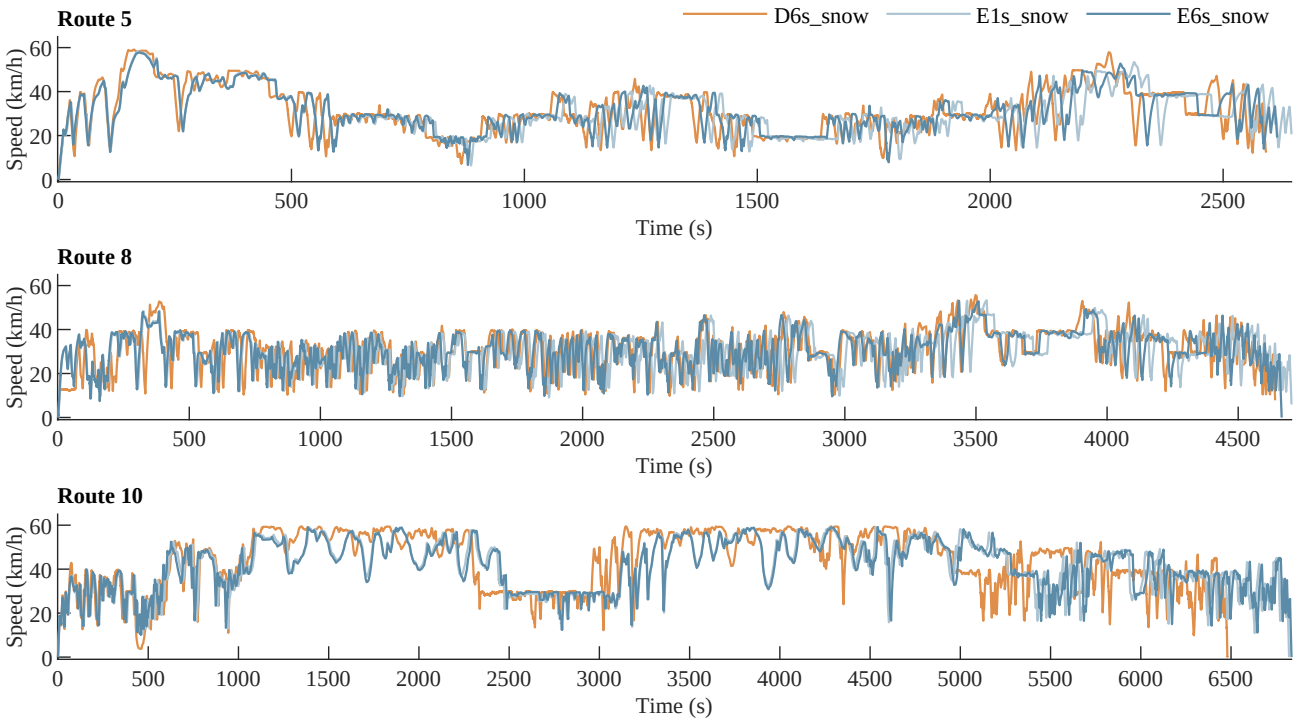

Figure 12. Simulated speeds of three vehicle types with the snow load on routes 5, 8, and 10.

Figure 13 compares the time taken to drive each of the routes. As Figure 11 already indicated, differences in the total driving durations between the three powertrain types with the cargo profile are rather subtle. With the snow load the diesel version is consistently the fastest while the electric multi-speed and electric single-speed version come in the second and third. Nonetheless, even the biggest difference of about 6 minutes on Route 10 between D6s_snow and E1s_snow profiles alone would not be a bottle neck in this type of work case.

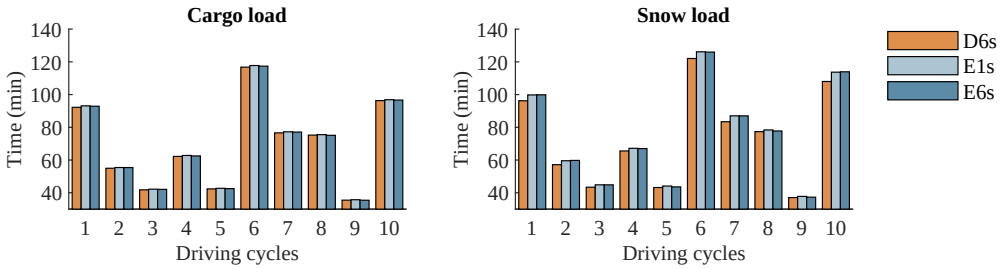

Figure 13. Total driving duration for each simulation in both load cases.

3.3.2. Electric Powertrain Efficiency

The diesel powertrain has inherently lower energy efficiency than the electric counterparts due to the ICE characteristics. Its maximum efficiency with a full engine load and nominal engine speed is only about 40%, which is not comparable with the electric powertrains with up to 97% efficiency. Simulated output efficiency graphs of electric vehicle profiles throughout the example routes 5, 8 and 10 are presented in Figure 14. Related graphs for all simulated routes are available in Appendix B—with the cargo load in Figure A5 and with the snow load in Figure A6.

One considerable result that appeared on all routes was that the average efficiency was constantly higher with the snow load than it was in the cargo cases. This stems from two reasons. First, the increased rolling resistance causes a higher load on the motor for longer periods of time and thereby results in higher efficiency with less fluctuation than

in the maximum mass scenario. This stands out especially during highway-speed regions which is the second reason. At speeds close to or higher than 60 km/h, both the speed and driving resistance increase the motor load, which occurs as higher efficiency. This is visible, for example, on Route 5 with the snow load (Figure 14). For kilometres 1–5 the speed request is higher than during the rest of the route.

Furthermore, the average efficiency of the electric multi-speed vehicle was higher than that of the single-speed vehicle on all routes. As Figure 6 points out, electric powertrain efficiency marginally decreases at speeds over the nominal. Additional gears help to maintain more constant and higher efficiency in spite of the speed variations, which allows the motor to rotate near its nominal speed and in its most optimal efficiency range. In contrast, the single-speed transmission forces the traction motor to run outside its most efficient region. This shows as efficiency drops when going uphill. Route 8, as an example, has plenty of hills during the first 20 km, which shows as larger efficiency range of the single-speed compared to the corresponding multi-speed profiles (Figure 14). Although electric powertrains possess high efficiency, even small dips affect the energy consumption and overall performance.

Route 10, with the highest average speed, is a good example on how the efficiency of the single-speed cargo load case is significantly lower for kilometres 10–30 and 35–75, while the corresponding multi-speed vehicle efficiency remains stable due to the additional gears which allow the motor to rotate in a more optimal operating range (Figure 14). This is less significant in the cargo scenarios on routes 5 and 8 which contain fewer highway speed sections.

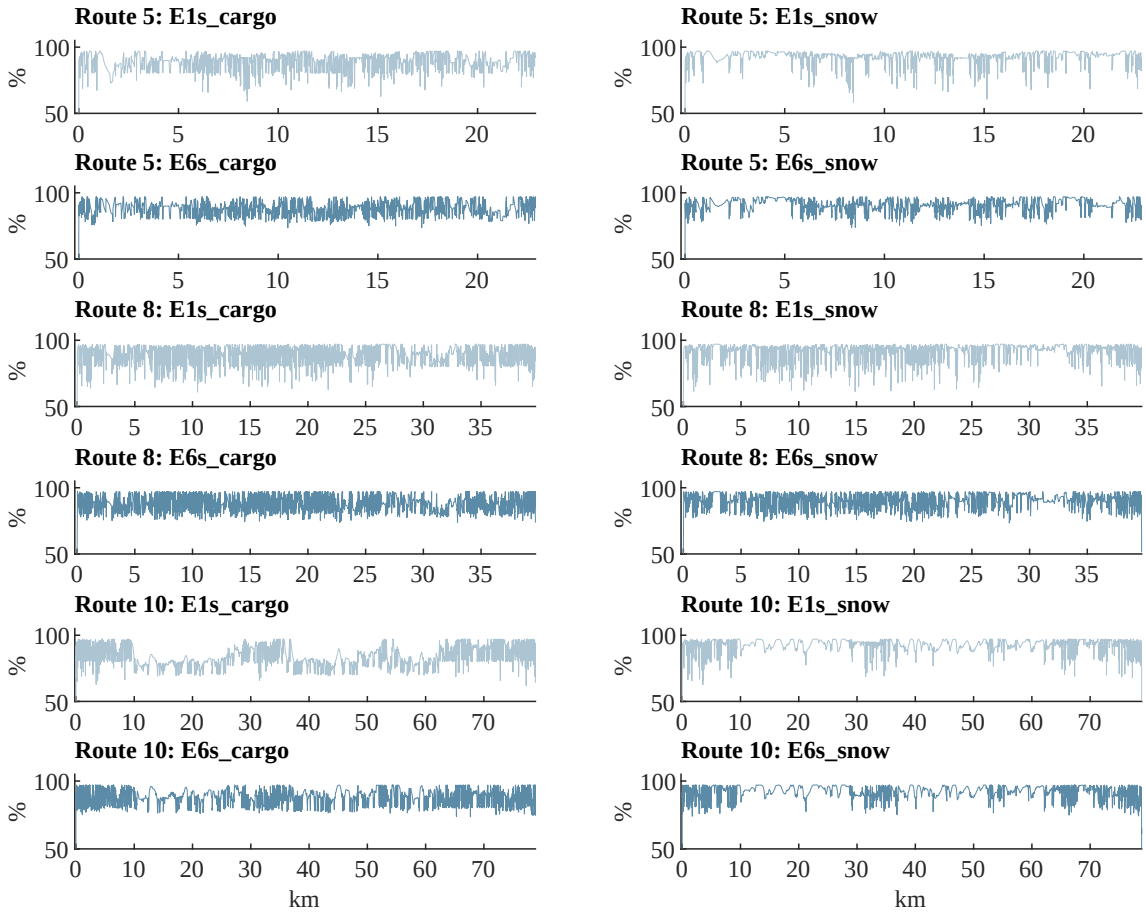

Figure 14. Simulated powertrain efficiency for the electric vehicles throughout driving cycles 5, 8, and 10. The graphs on the left describe the cargo scenarios, whereas the graphs on the right show the snow load situations.

The efficiency performance results indicate that the powertrain efficiency is strongly influenced by the road slope and speed characteristics. Both incur sudden drops on the efficiency graphs. The multi-speed profiles clearly manage to compensate for these better with the gear changes.

3.3.3. Consumption Performance

The total energy flow in each powertrain was obtained through the mechanical work by integrating the motor and engine power between the traction machine and the transmission. Table 6 lists the total energy flow in the positive (from motor to transmission) and the negative (from transmission to the motor) directions. The latter for the diesel powertrain describes the engine braking energy that is lost in the process, whereas in EV powertrains it stands for regenerative braking energy which can be stored in the battery.

Table 6. The total energy flow between the engine or motor and the transmission calculated through mechanical work. Energy values are divided into positive and negative values. Latter in the diesel case represents engine braking and regenerated braking in electric cases.

Route	D6s_cargo pos./neg. [kWh]	E1s_cargo pos./neg. [kWh]	E6s_cargo pos./neg. [kWh]	D6s_snow pos./neg. [kWh]	E1s_snow pos./neg. [kWh]	E6s_snow pos./neg. [kWh]
1	113/−13	103/−40	106/−45	219/−5	208/−10	214/−12
2	67/−8	62/−24	63/−25	133/−2	127/−5	130/−7
3	49/−6	45/−17	46/−19	96/−2	91/−4	94/−5
4	70/−10	63/−27	65/−31	134/−4	127/−6	131/−8
5	39/−6	34/−15	36/−18	75/−3	71/−3	74/−5
6	133/−20	120/−49	124/−55	255/−8	242/−11	249/−14
7	91/−11	83/−28	85/−31	186/−5	177/−6	181/−7
8	85/−14	74/−37	78/−44	137/−7	127/−10	132/−14
9	41/−7	36/−16	37/−19	72/−3	66/−4	68/−5
10	119/−14	109/−33	111/−35	257/−5	245/−5	251/−7

Table 6 shows that the disparity between the positive energy flow of all vehicle profiles is rather minor per route and per load case, which means that the vehicles have made the same amount of driving work. This also supports the comparability between the different simulation runs. It is reasonable, however, that the electric vehicles with less powerful powertrains result in a slightly smaller speeds and aerodynamic drag and hence, less work done in the drivetrain than the diesel version. Furthermore, the regenerated energy of the cargo load profile is constantly higher compared to the snow load profiles. This is because the additional driving resistance from the ploughing equipment drains the energy so that less can be regenerated.

Note that the calculated mechanical work describes the energy flow at the particular point between the traction machine and the transmission. This means that the energy flow from the battery needs to be higher than the positive flow values in Table 6 to cover the losses. In the same way, not all of the regenerable negative energy flow is conveyed all the way to the battery.

In our simulation model, the total energy consumption is calculated from the energy source (a fuel tank or a battery). We follow the tank-to-wheel principle where the energy at the beginning is the energy content of the energy source which is compared to the end situation. Table 7 lists the average consumption per 100 km for all simulation cases.

Table 7. Simulated average consumption values per 100 km, where the first three columns are from the cargo load cases and the last three columns from the snow load cases. The diesel consumption is represented in litres and the energy consumption in kWhs.

Route	D6s_cargo [L/100 km]	E1s_cargo [kWh/100 km]	E6s_cargo [kWh/100 km]	D6s_snow [L/100 km]	E1s_snow [kWh/100 km]	E6s_snow [kWh/100 km]
1	43	128	129	80	348	360
2	42	125	126	79	345	358
3	42	127	129	79	345	360
4	42	120	120	79	340	354
5	42	111	112	79	338	354
6	43	123	124	79	341	355
7	40	131	126	79	346	359
8	52	128	130	83	339	354
9	48	127	126	82	341	356
10	37	132	125	77	347	357

The diesel consumption is not directly comparable to the energy consumption, but to have a directive conception it was converted from L/100 km to kWh/100 km in Figure 15. The conversion is based on the generalisation that one litre of diesel fuel contains energy content of about 38 MJ which equals roughly 10 kWh.

A general conclusion that can be drawn from the average energy consumption values is that snow ploughing with the 20-ton truck consumes at least twice as much compared to the 28 ton cargo load in all simulation cases (Figure 15). After the rough conversion from litres to kWhs, the diesel vehicle energy consumption is still two times higher compared to the EVs in both the cargo and snow load scenario.

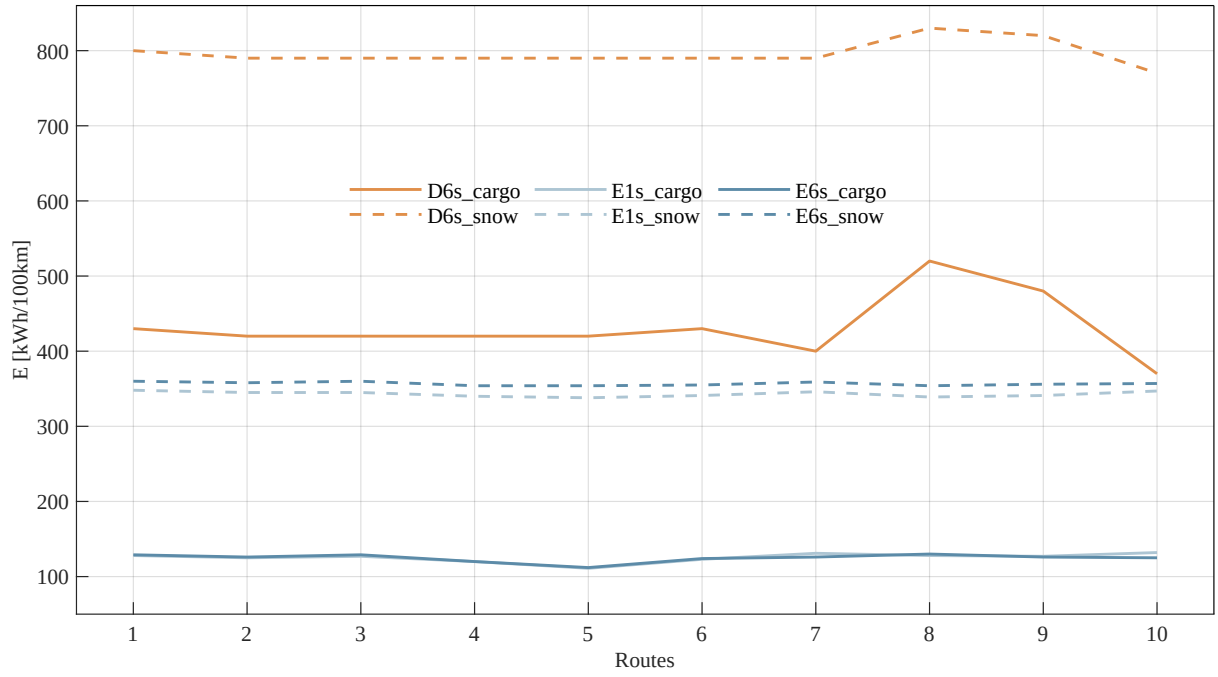

Figure 15. Simulated average consumptions where diesel consumption values are converted to kWh/100 km.

It was also noticeable that the average speed had a clear impact on the average consumption of the diesel powertrain, especially with the cargo load. ICEs are the most energy efficient at highway speeds and accordingly the lowest average consumption values of the diesel profiles were obtained on routes 7 and 10 (Figure 15). However, due to speeds over 60 km/h been eliminated from the snow load cases, the phenomena is more subtle

with D6s_snow. In contrast, routes 8 and 9 with the lowest average speeds produced the highest average consumptions. This was not similarly visible in the EV results because of their high efficiency throughout the whole speed range.

In the cargo scenario the electric single-speed consumed slightly less or as much as the multi-speed truck on most routes as their average speeds were almost the same per route. The remained difference is explained by the total final drive efficiency coefficient that was 0.96 for the single-speed and 0.94 for the multi-speed. Only routes 7 and 10 with the highway speed segments were the exceptions where the electric single-speed consumed more than the multi-speed because its motors is forced to less efficient operating range. In practice, the difference in electric powertrain consumptions with the cargo load is significant only when highway speeds are necessitated.

Then again, in the snow load scenario the electric multi-speed version appears to consume notably more than the single-speed. One reason is the same than in the cargo load case that the higher final drive efficiency results in lower consumption than with the multi-speed profile. The second reason is that because of the lack of available tractive forces, the single-speed is slightly slower than the multi-speed version and therefore it also consumes less.

4. Discussion and Conclusions

We simulated an e-retrofitted heavy-duty truck with and without a multi-speed transmission to assess its dynamic performance during high-load working cycles. The simulations were based on a real e-retrofit project, where a commercial diesel truck was converted to electric. By comparing the traction performance of the diesel version to the electrical configurations, we evaluated the viability of retaining the gearbox and torque converter from the original powertrain. Two types of load scenarios, namely a cargo load with the maximum payload and snow ploughing with increased resistive forces, were studied. Ten driving cycles for realistic routes were accomplished based on map information of the route curvature, altitude, speed limits, and other characteristics. The VTT Smart eFleet simulation toolbox was used for creating the driving cycles and running the simulations.

In the light of our results, the six-speed transmission from the original diesel truck is applicable for the e-retrofitted powertrain in heavy load working conditions. Even though the single-speed traction performance was not comparable to the multi-speed vehicles, it still executed all routes tolerably in the both loading scenarios. However, the single-speed occasionally struggled with overcoming the steeper hills and reaching the highway speeds, which appeared as a slower average speed compared to the other vehicle profiles. The simulations indicate that the multi-speed transmission has the biggest effect on the traction performance. The gearbox supplies the maximum power throughout the whole operating speed range ensuring higher tractive forces under high load working cycles. It also significantly improved the powertrain efficiency throughout the whole operating speed range, particularly at the highway speeds. The multi-speed transmission had some impact on the energy consumption as well. Due to the higher final drive efficiency of the single-speed, it consumed equally or slightly less than the multi-speed truck with the cargo load on most routes. On routes including highway speeds, the single-speed was less energy efficient than the multi-speed. Additionally, the slower average speed of the single-speed version with the snow load stood out as a notably lower average consumption compared to the multi-speed profile. We summarise these results from the multi-speed transmission as follows. To summarise, the multi-speed transmission:

- significantly improves the traction performance and the overall powertrain efficiency;
- slightly improves the speed performance in terms of the acceleration capability;
- has only a minimal effect on the energy consumption of the electric heavy-duty truck;
- generally improves the dynamic performance of a heavy-duty truck, which supports exploiting the original gearbox.

When comparing our results to the previous studies, we stand out by the realistic comprehensive set of driving cycles which enable a more reliable evaluation of the heavy-

duty vehicle performance. We also studied snow ploughing as a new type of working cycle and addressed its special requirements for the powertrain. From the e-retrofitting perspective, the benefit of a gearbox, originally designed as part of the diesel transmission, was demonstrated.

The maximum battery power of 194 kW distinctly limited the maximum speed for the electric profiles. The available battery power also compromised the acceleration performance of the electric trucks, which led to the increased driving durations. In case more reactive or faster performance is required, either the torque converter could be unlocked to temporarily provide extra torque, or the battery system management could be adjusted to allow higher power peaks for short periods. At this point, neither of the options were investigated, but both could be considered as potential objectives in the future.

To simplify our simulations, we made some general assumptions regarding the total vehicle mass and load parameters. In reality, an e-retrofitted vehicle would weigh more than the original diesel version due to heavy electrical components, and the transmission parts in a multi-speed vehicle add additional mass in comparison to a single-speed version. We assumed that all cargo load profiles weigh 28 tons and the snow load profiles 20 tons, which needs to be considered when interpreting the results. In addition, our load cases were simulated using rather extreme values to assess the driving performance properly. In practise all load parameters are rarely at their maximum simultaneously, which is why the total consumption values are probably moderately overestimated in our simulations.

The experimental e-retrofitting of the diesel truck is currently in progress. Once the powertrain renovation is finished, there is a possibility to measure its technical performance using telemetry equipment while the vehicle is driven in daily use. The received measurement data could then be used to further validate our simulation model.

Author Contributions: Conceptualisation, M.V., P.R., J.K., J.P.-M. and M.P.; methodology, M.V. and P.R.; software, M.V. and P.R.; validation, M.V., P.R. and J.P.; formal analysis, M.V. and P.R.; investigation, M.V. and P.R.; resources, M.P.; writing—original draft preparation, M.V., P.R., J.K. and J.P.-M.; writing—review and editing, M.V., P.R., J.K., J.P.-M., M.P., J.P., K.T. and A.B.; visualisation, M.V. and P.R.; supervision, M.P. and A.B.; project administration, M.P. and J.K.; funding acquisition, M.P. All authors have read and agreed to the published version of the manuscript.

Funding: This research was supported by the mySMARTLife project funded by the European Union's Horizon 2020 Research and Innovation Programme, grant number 731297.

Acknowledgments: This research have been made in parallel with a real electric retrofit process performed by Tampere University of Applied Sciences for a vehicle of Helsinki City Construction Services (Stara) with funding via Forum Virium Helsinki Ltd. We thank all the mentioned partners for collaboration and providing input data for this study. Further, we thank Joel Anttila (VTT Technical Research Centre of Finland) for his valuable comments that greatly improved the manuscript.

Conflicts of Interest: The authors declare no conflict of interest. The funders had no role in the design of the study; in the collection, analyses, or interpretation of data; in the writing of the manuscript, or in the decision to publish the results.

Appendix A. Simulated Speed Performance Results

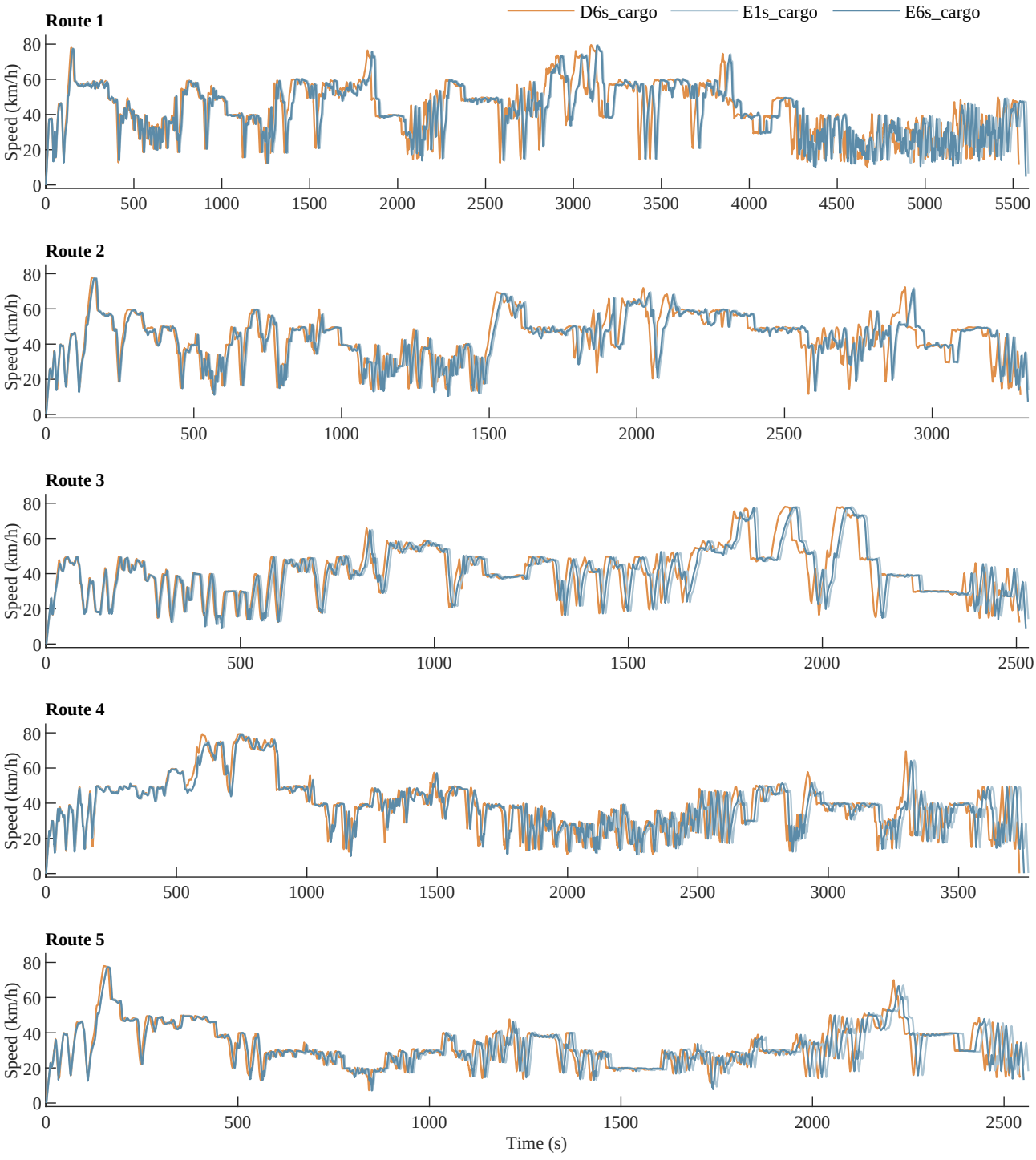

Figure A1. Speed performance with the cargo load on routes 1–5.

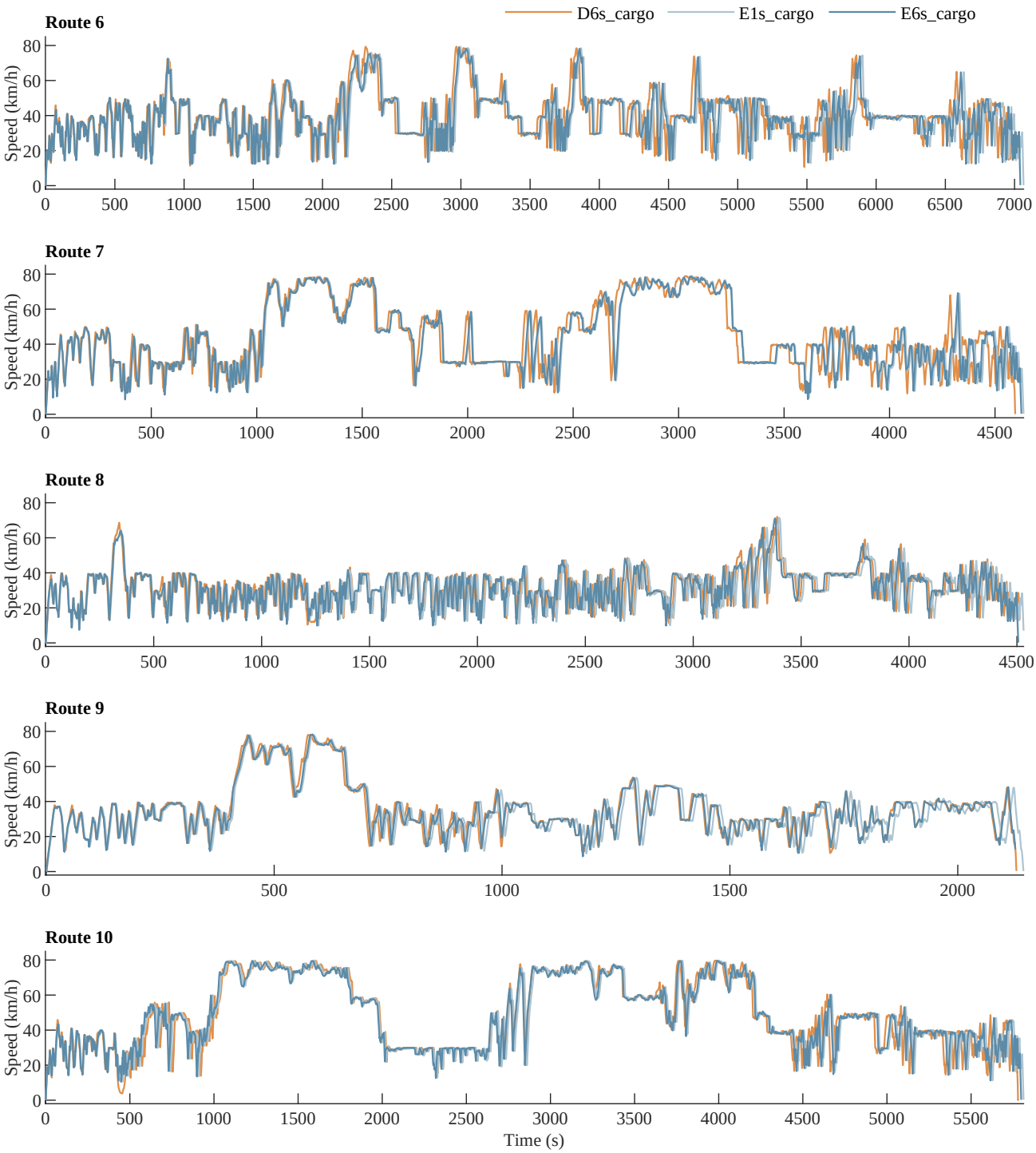

Figure A2. Speed performance with the cargo load on routes 6–10.

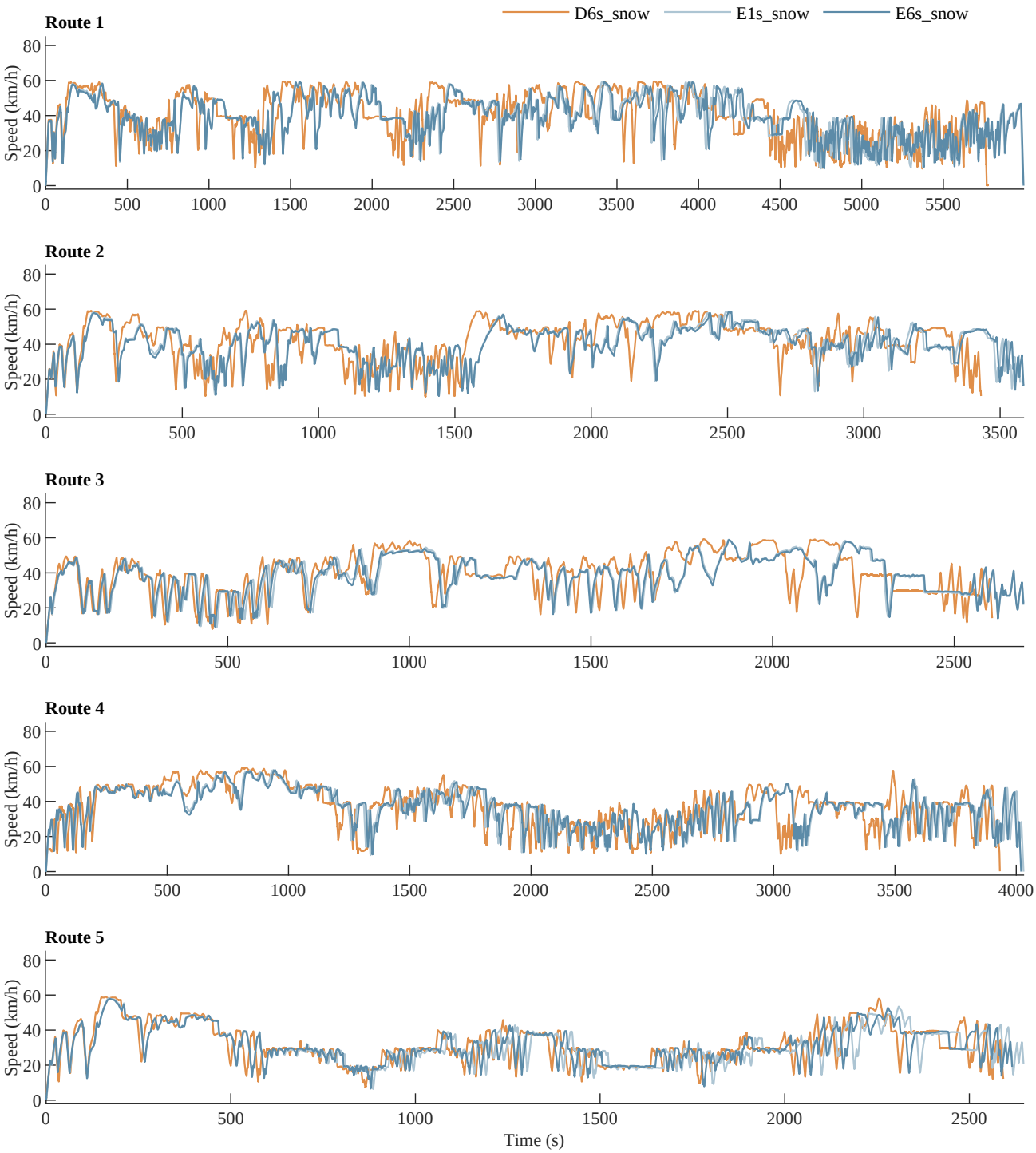

Figure A3. Speed performance with the snow load on routes 1–5.

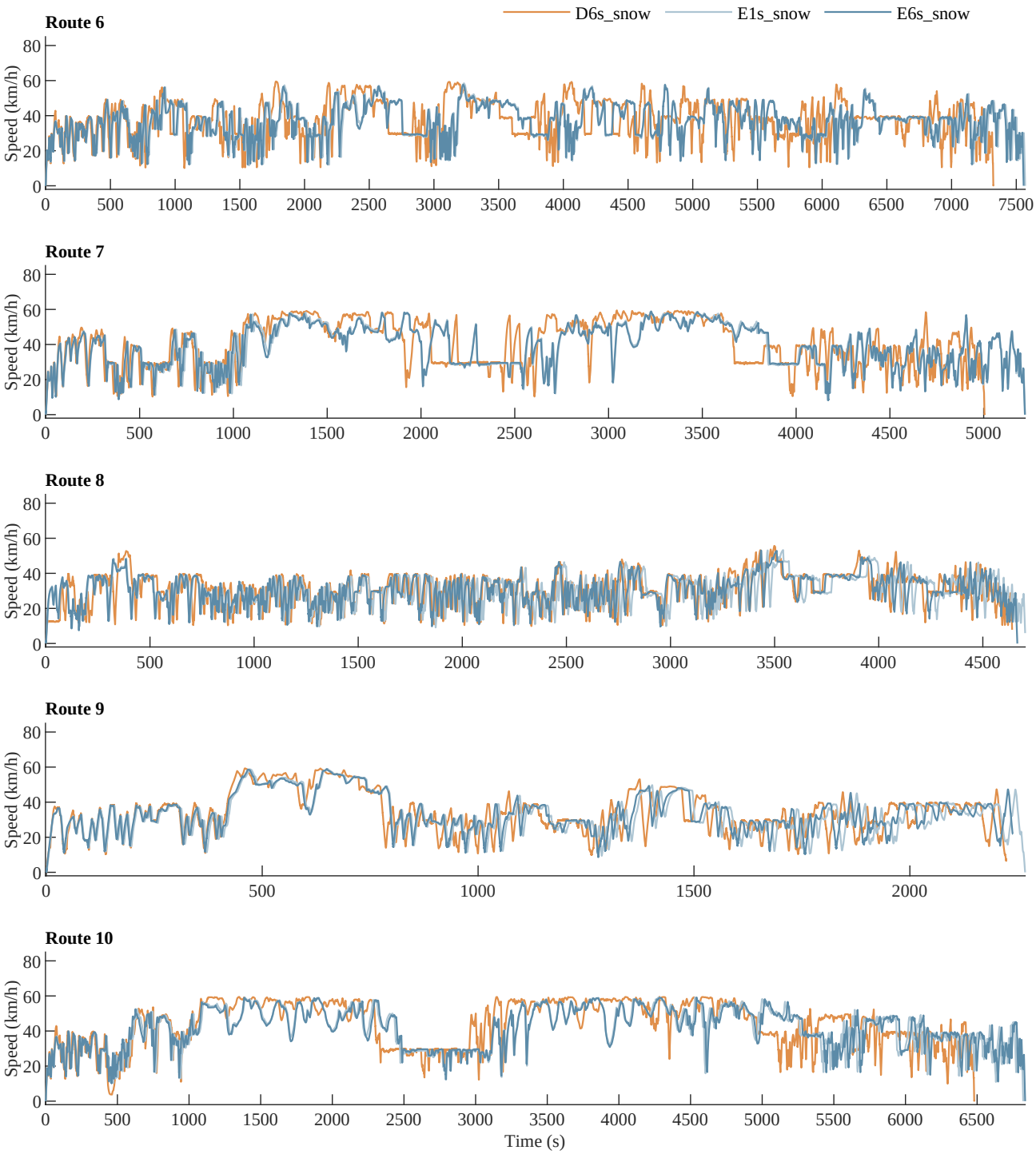

Figure A4. Speed performance with the snow load on routes 6–10.

Appendix B. Simulated Powertrain Efficiency Results

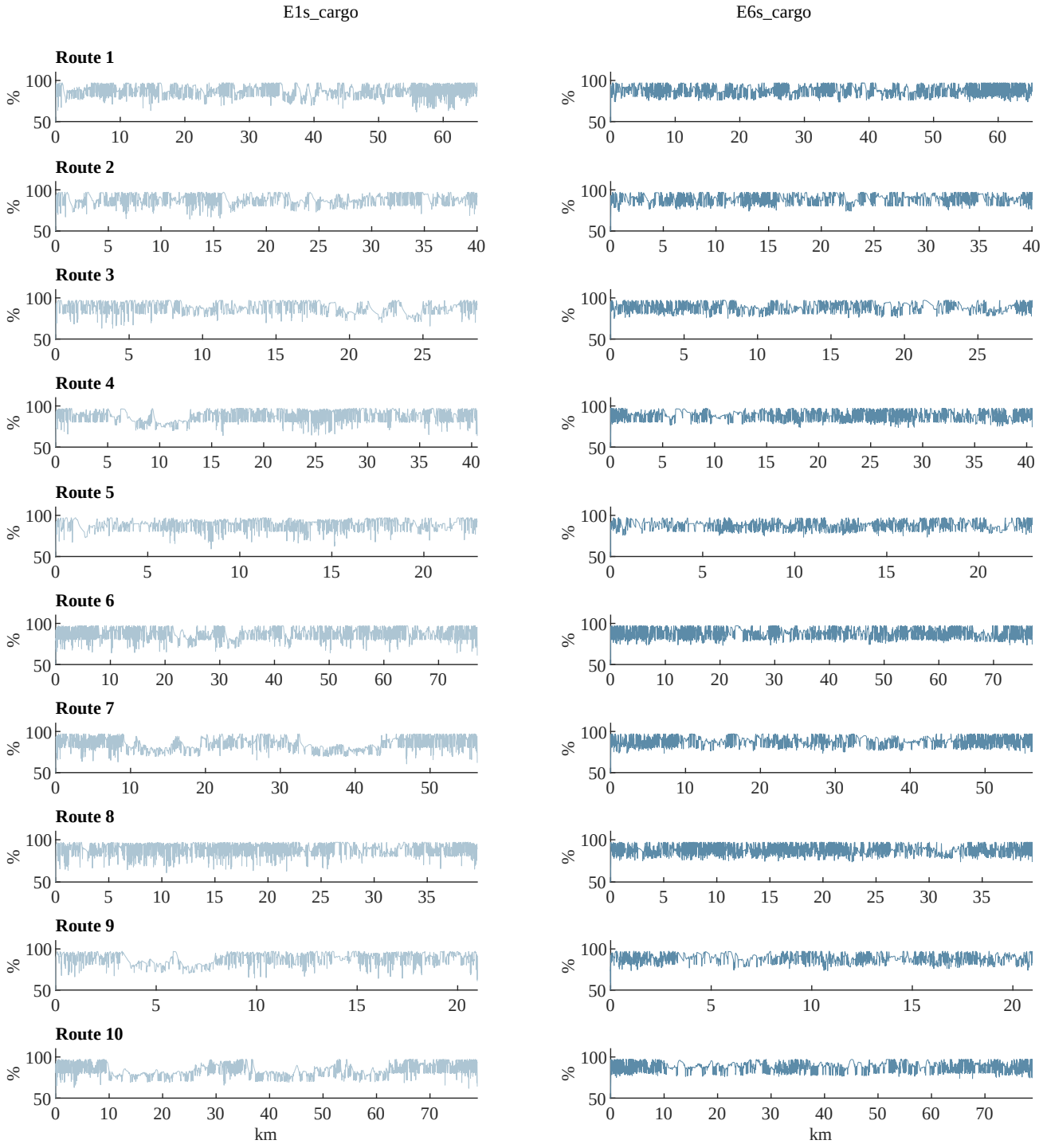

Figure A5. Electric powertrain efficiency with the cargo load on routes 1–10.

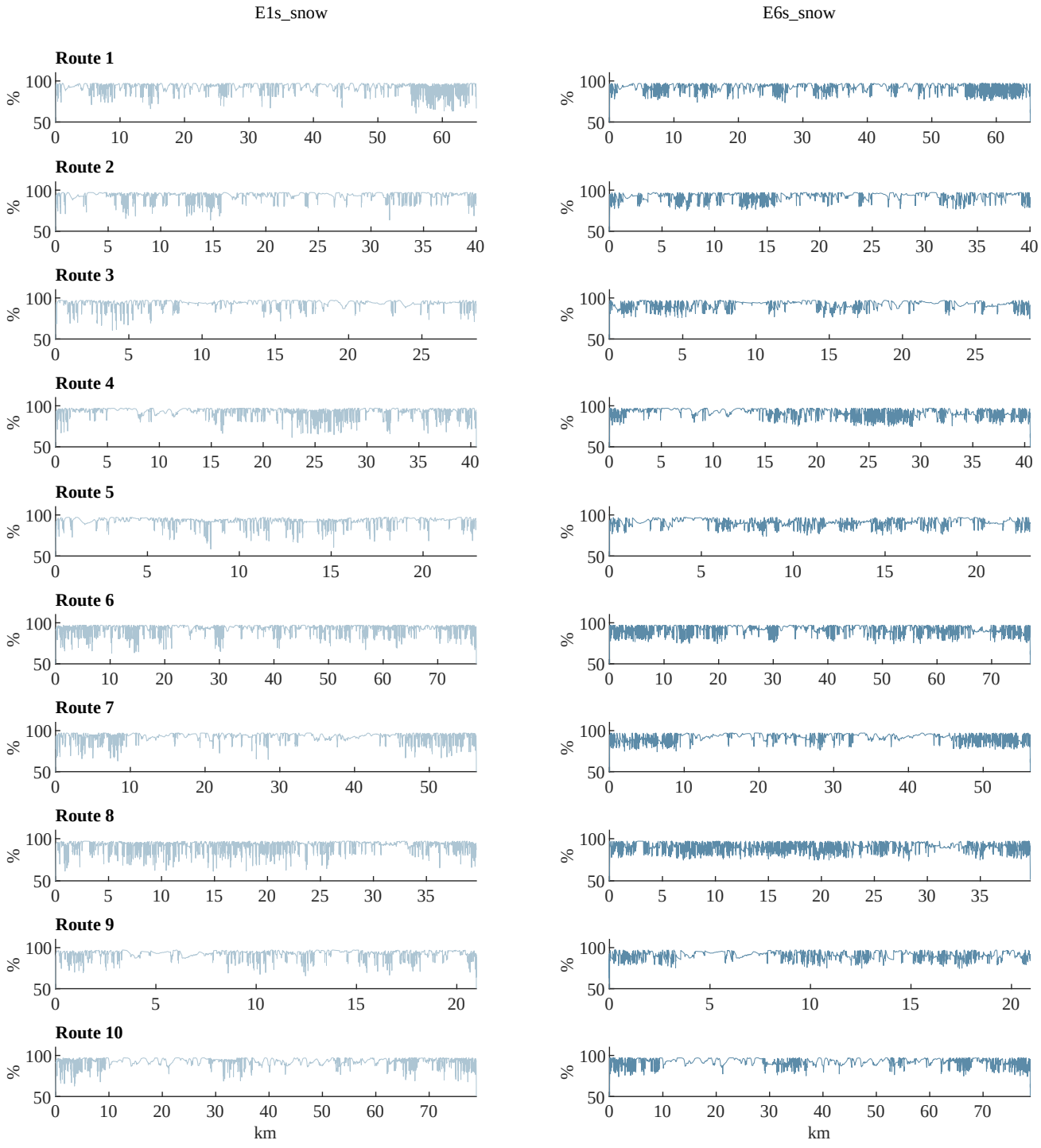

Figure A6. Electric powertrain efficiency with the snow load on routes 1–10.

References

1. Betsi-Argyropoulou, I.I.; Moschovi, A.M.; Polyzou, E.N.; Yakoumis, I. Towards Ammonia Free Retrofitting of Heavy-Duty Vehicles to Meet Euro VI Standards. In *Vehicle and Automotive Engineering 3*; Jármai, K., Voith, K., Eds.; Springer: Singapore, 2021; pp. 206–221. [CrossRef]
2. Lombardi, S.; Villani, M.; Bella, G.; Tribioli, L. *Retrofit of a Heavy-Duty Diesel Truck: Comparison of Parallel and Series Hybrid Architectures with Waste Heat Recovery*; SAE International: Warrendale, PA, USA, 2020. [CrossRef]

3. European Union. *Regulation (EU) 2019/1242 of the European Parliament and of the Council of 20 June 2019 Setting CO_2 Emission Performance Standards for New Heavy-Duty Vehicles and Amending Regulations (EC) No 595/2009 and (EU) 2018/956 of the European Parliament and of the Council and Council Directive 96/53/EC*; European Commission. OJ L198/202; European Union: Brussels, Belgium, 2019.
4. Linkker Intelligent Mobility. Accelerating Emission Reductions: Linkker Diesel to Electric Bus Conversion Kits. Available online: http://www.linkkerbus.com/2020/press-release/accelerating-emission-reductions-linkker-diesel-to-electric-bus-conversion-kits/ (accessed on 23 February 2022).
5. E–Trofit. Pepper Motion GmbH—Electrifying Transportation. Available online: https://www.peppermotion.com/en/ (accessed on 12 January 2022).
6. Hoeft, F. Internal combustion engine to electric vehicle retrofitting: Potential customer's needs, public perception and business model implications. *Transp. Res. Interdiscip. Perspect.* **2021**, *9*, 100330. [CrossRef]
7. Karki, A.; Shrestha, B.P.; Tuladhar, D.; Basnet, S.; Phuyal, S.; Baral, B. Parameters Matching for Electric Vehicle Conversion. In Proceedings of the 2019 IEEE Transportation Electrification Conference (ITEC-India), Bengaluru, India, 17–19 December 2019; pp. 1–5. [CrossRef]
8. Ahssan, M.; Ektesabi, M.; Asghari Gorji, S. Electric Vehicle with Multi-Speed Transmission: A Review on Performances and Complexities. *SAE Int. J. Altern. Powertrains* **2018**, *7*, 169–181. [CrossRef]
9. Hofman, T.; Dai, C.H. Energy efficiency analysis and comparison of transmission technologies for an electric vehicle. In Proceedings of the 2010 IEEE Vehicle Power and Propulsion Conference, Lille, France, 1–3 September 2010; pp. 1–6. [CrossRef]
10. Morozov, A.; Humphries, K.; Zou, T.; Rahman, T.; Angeles, J. Design, Analysis, and Optimization of a Multi-Speed Powertrain for Class-7 Electric Trucks. *SAE Int. J. Altern. Powertrains* **2018**, *7*, 27–42. [CrossRef]
11. Verbruggen, F.J.R.; Rangarajan, V.; Hofman, T. Powertrain design optimization for a battery electric heavy-duty truck. In Proceedings of the 2019 American Control Conference (ACC), Philadelphia, PA, USA, 10–12 July 2019; pp. 1488–1493. [CrossRef]
12. European Union. *Regulation of the European Parliament and of the Council on the Monitoring and Reporting of CO_2 Emissions from and Fuel Consumption of New Heavy-Duty Vehicles*; European Commission. 2017/0111 (COD); European Union: Brussels, Belgium, 2017.
13. Tan, S.; Yang, J.; Zhao, X.; Hai, T.; Zhang, W. Gear Ratio Optimization of a Multi-Speed Transmission for Electric Dump Truck Operating on the Structure Route. *Energies* **2018**, *11*, 1324. [CrossRef]
14. Ritari, A.; Vepsäläinen, J.; Kivekäs, K.; Tammi, K.; Laitinen, H. Energy Consumption and Lifecycle Cost Analysis of Electric City Buses with Multispeed Gearboxes. *Energies* **2020**, *13*, 2117. [CrossRef]
15. VTT Technical Research Centre of Finland Ltd. Design Zero-Emission Transport Systems with VTT Smart eFleet Service. Available online: https://www.vttresearch.com/en/ourservices/design-zero-emission-transport-systems-vtt-smart-efleet-service (accessed on 8 February 2022).
16. Halmeaho, T.; Rahkola, P.; Pellikka, A.P.; Ruotsalainen, S.; Tammi, K. Electric City Bus Energy Flow Model and Its Validation by Dynamometer Test. In Proceedings of the 2015 IEEE Vehicle Power and Propulsion Conference (VPPC), Montreal, QC, Canada, 19–22 October 2015; pp. 1–6. [CrossRef]
17. Ranta, M.; Karvonen, V.; Potter, J.J.; Pasonen, R.; Pursiheimo, E.; Halmeaho, T.; Ponomarev, P.; Pihlatie, M. Method including Power Grid Model and Route Simulation to Aid Planning and Operation of an Electric Bus Fleet. In Proceedings of the 2016 IEEE Vehicle Power and Propulsion Conference (VPPC), Hangzhou, China, 17–20 October 2016; pp. 1–5. [CrossRef]
18. Anttila, J.; Todorov, Y.; Ranta, M.; Pihlatie, M. System-Level Validation of an Electric Bus Fleet Simulator. In Proceedings of the 2019 IEEE Vehicle Power and Propulsion Conference (VPPC), Hanoi, Vietnam, 14–17 October 2019; pp. 1–5. [CrossRef]
19. Wong, J.Y. *Theory of Ground Vehicles*; John Wiley & Sons: New York, NY, USA, 1993.
20. Paterlini, G.; Yucel, S. *Rolling Resistance Validation*; Technical Report; Minnesota Department of Transportation: St Paul, MN, USA, 2015.